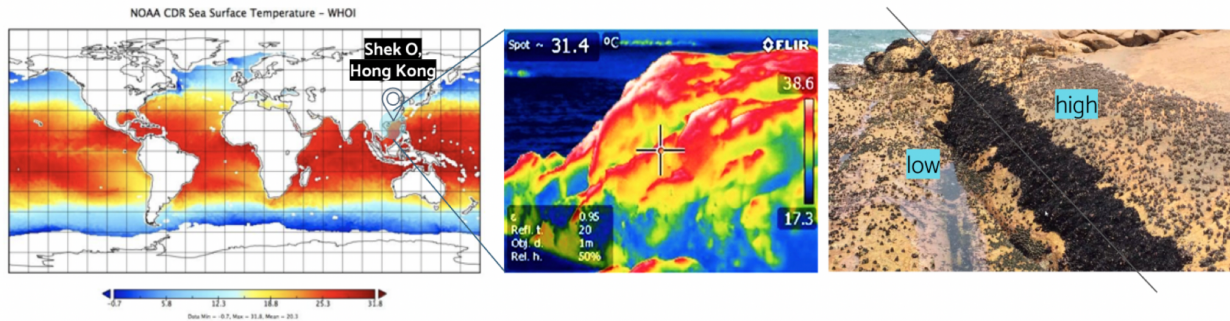


## Do warming rates influence functional and genetic regulation of thermal stress in intertidal mussels? Insights for climate change and extreme events



Author:  
 Debbie Leung  
 Columbia University in the City of New York  
 Department of Ecology, Evolution and Environmental Biology

Research Mentors:  
 Juan Diego Gaitán-Espitia, Swire Institute of Marine Science, University of Hong Kong  
 (jdgaitan@hku.hk)  
 Gray A. Williams, Swire Institute of Marine Science, University of Hong Kong  
 (hrsbwga@hku.hk)

Research Advisor:  
 Hugh Ducklow, Lamont Doherty Earth Observatory, Columbia University  
 (hducklow@ldeo.columbia.edu)

**TABLE OF CONTENTS**

<b>ABSTRACT</b>	<b>3</b>
<b>INTRODUCTION</b>	<b>4</b>
<b>MATERIALS AND METHODS</b>	<b>9</b>
2.1 Animal collection and acclimation conditions	9
2.2 Warming Experiments	9
2.3 Physiological Measurements	11
2.4 Genetic Measurements	11
<b>RESULTS</b>	<b>13</b>
3.1 Physiological Analysis	13
3.2 Genetic Analysis	19
3.2.1 De Novo Assembly	19
3.2.2 Functional Annotation	20
3.2.3 Differential Gene Expression	21
<b>DISCUSSION</b>	<b>28</b>
4.1 Transition from Water to Air	28
4.2 Impact of Warming Rates	30
4.2.1 Rapid Stress Response	30
4.2.2 Acclimation Response	32
4.3 Adaptive Capability of Shore Populations	34
4.4 Coupling of Physiological and Genetic Mechanisms	36
<b>CONCLUSIONS</b>	<b>38</b>
<b>RECOMMENDATIONS</b>	<b>39</b>
<b>ACKNOWLEDGEMENTS</b>	<b>41</b>
<b>SUPPLEMENTARY FIGURES</b>	<b>42</b>
<b>SUPPLEMENTARY TABLES</b>	<b>47</b>
<b>REFERENCES</b>	<b>52</b>

**ABSTRACT**

The interaction of thermal and desiccation conditions with small-scale physical features of a habitat may determine the thermal tolerance of organisms. In one of the most stressful and fluctuating habitats such as the tropical rocky shores, a gradient of temperature variations develops along the vertical profile from the high shore to the subtidal that may be governed by the rate of temperature change. This study focuses on the physiological and molecular mechanisms of thermoregulation of the mid-shore intertidal purplish bifurcate mussel *Mytilisepta virgatus* by addressing (1) how varying warming rates affect their physiological performance and gene expression during rapid heating and acclimation and (2) how this relationship may differ between shore populations within the same mussel bed. Using heat ramping experiments, we examined four physiological variables of interest: heart rate, osmolality, weight loss percentage and characterized gene expression profiles. Faster rates significantly decreased weight loss and average thermal equilibrium but did not show changes in heart rate and osmolality. Higher protein-folding genes were upregulated at the expense of pro-survival pathways. Higher-shore populations displayed similar patterns at the fast rate with higher protein folding gene expression, faster signaling activation and transduction as well as stronger repair and immune ability against heat stress. As physiological indicators may not have the resolution to reflect minute changes in molecular machinery in response to thermal stress, an integrative approach that incorporates molecular techniques in physiological studies can provide important insights into the effect of warming rates on sessile intertidal communities.

## 1. INTRODUCTION

Tropical rocky shores inhabit the interface between marine and terrestrial environments and are one of the most extreme environments on Earth (Moyen et al., 2019). Organisms living in tropical intertidal rocky shores are continuously exposed to a combination of thermal and desiccation stress during tidal emersion including high temperature fluctuations, dehydration and oxygen deprivation (Freire et al., 2011; Rolán-Alvarez et al., 2015). For marine ectotherms with limited ability to behaviourally thermoregulate, fluctuations in environmental temperature can be a major challenge. Their body temperature, being highly dependent on environmental temperature, affects all aspects of their performance and survival (Angilletta et al., 2002). Consequently, marine ectotherms have been shown to be living close to physiological limits (Plinsky et al., 2019; Somero, 2010). Those inhabiting tropical intertidal rocky shores are even more vulnerable as they are continually exposed to tidal changes and temperature fluctuations that can vary from 15 to 45 °C on a summer day (Williams and Morritt 1995).

Previous studies have often focused on using average temperature changes to assess the sensitivity of intertidal ectotherms and predict their ecological responses to climate change. However, this approach obscures the importance of weather (short-term local patterns), climate (long-term broad-scale trends) and the interactive effects of climatic and non-climatic stressors. A mechanistic process-based understanding of which factors affect organisms most and how is required to accurately forecast species-specific responses to local variability in environmental conditions (Helmuth et al., 2014). In particular, warming rate has been implicated in organismal ability to acclimate to high temperatures, resulting in differential biological responses (Peck et al., 2009). Differences between animals from environments that experience different levels of temperature variability suggest that the physiological mechanisms underlying thermal sensitivity may vary at different rates of warming. (Nguen et al., 2011). Though some marine ectotherm populations may have the plasticity to acclimate to small temperature changes, extreme events with drastic temperature changes can cause metabolic failure (WetHEY et al., 2011). While it has been well established that the body temperatures of intertidal ectotherms are influenced by both sea surface temperature and aerial temperature, the effects of the aerial versus seawater temperature are not well delineated (Place et al., 2008). As most studies to date have conducted warming rates in water (Nguyen et al., 2011), we aim to elucidate the effects of warming rates in air on the thermal performance of intertidal ectotherms.

In response to varying warming rates in the environment, variations in intertidal ectotherms' warming rates have been recorded in field studies depending on whether the shore is wave-exposed or wave-protected (Denny et al., 2011). Body warming rates are also found to vary depending on the tidal height of the organisms on the shore. Miller and Dowd (2017) reported that high-shore mussels experienced faster average daily heating rates ( $6.79^{\circ}\text{C h}^{-1}$ ) than

low-shore mussels ( $1.32^{\circ}\text{C h}^{-1}$ ), with maximum heating rates as fast as  $20^{\circ}\text{C h}^{-1}$  and  $12^{\circ}\text{C h}^{-1}$  respectively. Moyen et al. (2019) compared heart rates between the high and low shore populations of *Mytilus californianus* with different emersion durations and mean daily heating rates and concluded the heart rates of the high shore populations precipitously declined at a significantly lower temperature. Similarly, Gracey et al. (2008) revealed there were significant gene expression differences in the physiological states experienced by *M. californianus* based on their vertical position on the shore due to variation in abiotic stress along the rocky intertidal zone.

Despite living close to their thermal tolerance limits and experiencing varying warming rates in the environment, tropical intertidal organisms have acquired physiological and genetic mechanisms that allow for local adaptation to these extreme thermal conditions (Han et al., 2020). Sessile intertidal ectotherms, in particular, develop the adaptive strategy of metabolic depression to enhance survival for prolonged periods of environmental stress (Storey and Storey, 2004). As part of this response, both physiological (heart and respiration rates, water loss, etc.) and cellular processes (transcription, translation, cell cycle, etc.) are actively suppressed (Storey and Storey, 2005).

Thermal tolerance of ectotherms has often been assessed in the laboratory by monitoring cardiac physiology through heart rate (Logan et al., 2012). In a typical setup, ectotherms are heated at a certain rate ( $^{\circ}\text{C h}^{-1}$ ) until their heart rate drops rapidly, denoted as the heart's critical temperature ( $T_{\text{crit}}$ ) (Denny et al., 2011). While not acutely lethal,  $T_{\text{crit}}$  reflects the activation of a stress response that incurs cumulative cellular damage, including autophagy, apoptosis and inflammation (Storey and Storey, 2010) through the heating process. It has been observed that the expression of stress-related proteins, including heat-shock proteins, is upregulated at temperatures slightly below  $T_{\text{crit}}$  in mussels (Gracey et al., 2008) and protective genes and proteins are maximally expressed in limpets at  $T_{\text{crit}}$ . This suggests that cardiac dysfunction may result from a broad suite of underlying cellular mechanisms to thermal stress, such as heat-driven protein unfolding. Further increasing body temperature above  $T_{\text{crit}}$  is lethal and will lead to a cessation of heart rate, known as the flatline temperature. Similarly, osmotic stress is another physiological indicator through which ectotherms cope with temperature changes. It involves cell volume regulation through changes in intracellular amino acid and inorganic ion concentrations (Shumway and Freeman, 1984). In an attempt to osmoregulate, ectotherms isolate their soft tissues from the osmotically stressful environment with bivalves shutting their valves, gastropods withdrawing into their shells and closing the aperture with the operculum, and limpets clamping tightly to the rock (Morritt et al., 2007). Such isolation will limit oxygen uptake, leading to reduction of oxygen delivery to organs that accelerates the formation of reactive oxygen species (ROS) causing oxidative damage (Freire et al., 2011).

In response to the extreme prolonged temperature changes, ectotherms will enter a state of metabolic depression by suppressing aerobic metabolism and heart rate (Freire et al., 2011) as well as activating pro-survival pathways and controlled cell cycle regulation to slow down and repair cellular damage induced by stress (Falfushynska et al., 2020). Suppressing the rate of ATP consumption and production below the normoxic level, sometimes down to <5% of the standard aerobic metabolic rate, helps slow down the accumulation of potentially toxic end products and conserve energy reserves (Guppy and Withers, 1999; Shick et al., 2983; Sokolova et al., 2000). Other molecular mechanisms include reversible protein phosphorylation of key enzymes in signal transduction cascades (Storey and Storey, 2004; Storey and Storey, 2010; Koch, 2017) and gene activation or suppression via transcriptional, post-transcriptional and/or post-translational modifications (Biggar and Storey, 2015; Biggar and Storey, 2018; Hadj-Moussa et al., 2016; Storey, 2015; Wijenayake et al., 2018). Despite progress in our understanding of the functional regulation of metabolic depression, there are critical gaps in our knowledge of the interaction of ectotherms' physiological and molecular responses to thermal stress and their mechanisms underpinning this adaptive response.

This study aims to investigate [1] how varying warming rates modulate the physiological and molecular responses of sessile intertidal organisms to heat stress and [2] to what extent warming rates differentially affect populations at high and low intertidal shores with different exposure and microhabitat conditions using *Mytilisepta* (previously *Septifer*) *virgatus* (Figure 1). *M. virgatus* is a mid-shore wave-exposed sessile northern mussel species found near its southern limits in Hong Kong and has been recorded to regularly experience mass mortalities at its upper distributional boundary in summer due to high rock temperatures and low tides (Liu and Morton, 1995). Located in the mid-intertidal zone, *M. virgatus* can experience extreme rock temperatures exceeding 55°C (Cartwright and Williams, 2012; McAfee et al., 2018), where warming rates on rocks vary across the mussel bed with an average of 0.2°C/min (Williams, unpublished data). Given the variation of temperature change throughout the year, warming rates may account for the high-shore animals' mass mortalities as it affects how the organisms detect the coming change, prepare the physiological and metabolic adjustment, persist during the thermal stress, and recover afterwards. If they are not able to track the thermal change to keep up with their thermal equilibrium, they will most likely die.



Figure 1. *Mussel bed (black band) on a vertical shore gradient in Hong Kong. Photo taken in August 2020.*

This study hypothesizes that [1] warming rates in air affect *M. virgatus*' physiology and gene expression to prepare metabolic adjustments to cope with, persist through and recover from thermal stress (Figure 2). Faster warming rates result in shorter duration for organisms to mount mechanisms to respond to temperature changes, resulting in less drastic changes in physiology but higher gene expression related to stress and acclimation response. As metabolic depression is regulated by controlled gene expression of pro-survival pathways, heat stressed animals will show a transcriptional profile associated with fine regulation of protein degradation and inhibition of apoptosis among other pro-survival pathways. This transcriptional regulation of genes and the associated pathways will likely be differentially expressed at different warming rates. Fast warming rate results in lack of molecular control of metabolic pathways and an upregulation of genes related to thermal stress, such as ROS and heat shock protein production, while slow warming rate results in an upregulation of genes related to pro survival pathways.

Moreover, we also hypothesize that [2] the effect of warming rates is different between individuals within the same population. This is because thermal response (phenotypic plasticity) is context dependent, with individuals from the same population showing different responses depending on the degree of environmental variation they experience along the vertical shore gradient (Gleason *et. al.*, 2018; Miller and Dowd, 2017). Due to a higher phenotypic plasticity given the more extreme changes they experience in their environment, high-shore individuals demonstrate a greater repository of physiological and genetic changes and have a greater capacity to deal with faster warming rates as compared to individuals lower on the shore. Therefore, higher shore individuals are predicted to display greater changes in metabolic rate but lower stress response than lower intertidal sub-populations at high warming rates.

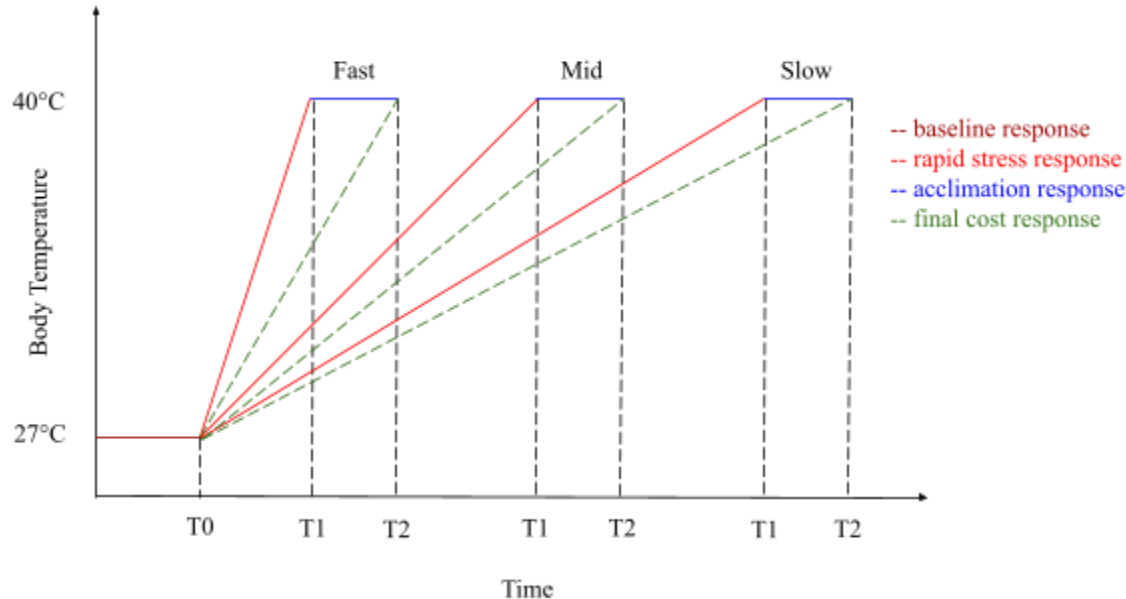


Figure 2. *Schematic of hypothesis and prediction (High and low-shore mussels heated from 27°C to 40°C at three different warming rates—0.1°C/min, 0.2°C/min and 1°C/min—display different rapid stress (red), acclimation (blue) and final cost responses (green). High-shore individuals are hypothesized to take shorter time to display full physiological and genetic changes compared to low-shore individuals.*

Understanding how physiological and cellular mechanisms are co-regulated by the rate of temperature change in air will yield important insights into the interaction of the functional and molecular regulation of metabolic depression in intertidal ectotherms when exposed to air. With tropical organisms being most vulnerable to temperature rise, it becomes increasingly necessary to predict potential responses to climate change and future extreme weather events. Investigating how warming rates approximating conditions when organisms are emersed affect regulation of thermal stress at both physiological and molecular levels as well as whether there is any phenotypic plasticity variation along the vertical shore gradient will advance such scientific efforts.

## 2. MATERIALS AND METHODS

### 2.1 Animal collection and acclimation conditions

Live *M. virgatus* between 35–45mm in shell length (> 1 year old) were collected from high (~ 1.5 m above C.D) and low shores (~ 0.7 m above C.D) of a wave-exposed coastline in Shek O, Hong Kong in the wet and hot season from June - September, 2020 (n = 140). Animals were placed in zip lock bags and transported within 1 hour to the aquarium in The University of Hong Kong. Before individually tagging the animals with nail polish to indicate their tidal height, any attached byssus threads or organisms on the mussel shells were removed. Mussels were randomly evenly separated into two tanks and maintained in four baskets (two per tank) submerged in unfiltered aerated seawater of 35 – 36ppt at ~27°C to mimic the mean sea surface temperature in summer. The tidal cycle where mussels are emersed during midday low tides from 2:00pm to 7:00pm was simulated using timers to control the pumping of water from a reservoir underneath. During the week of acclimation to remove effects of recent thermal history, mussels were fed with algae and tank water was changed once every two days.

### 2.2 Warming Experiments

To investigate the effects of warming rates on the physiology and gene expression of *M. virgatus*, three warming rates were chosen based on ecological relevance—0.1°C per min, 0.2°C per min and 1°C per min (Williams and Morritt, 1995). The factorial design of the experiment with the three factors of interest and their corresponding levels are diagrammed in Figure 3.

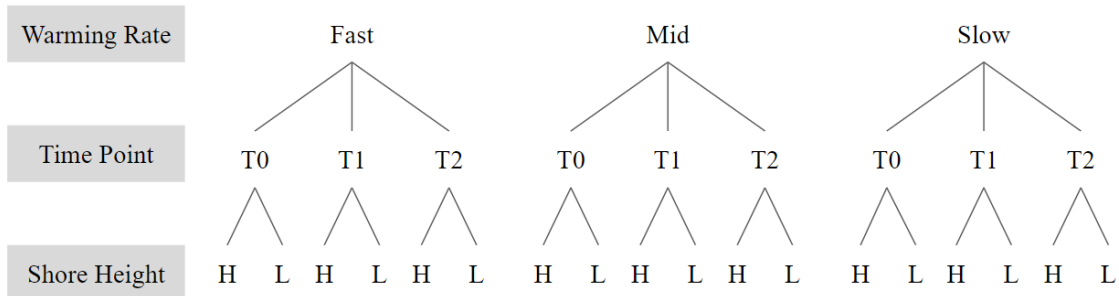


Figure 3. Factorial experimental design of three factors with fixed levels (three warming rates and two time points of two shore heights). T0 is considered control and the same samples are shared across all rates.

Each high and low shore mussel was randomly assigned into controls or one of the three treatments over the course of four days. To eliminate the effects of density on the animals, an equal number of mussels was selected from each basket for each round of the experiment. On the day of the experiments, mussels were first taken out of the tank and dried. They were

immediately measured for shell length ( $\pm 0.1\text{mm}$ ) and weighed for body weight ( $\pm 0.001\text{g}$ ). After attaching heart rate sensors, mussels were placed in a 200ml dry vial submerged in a programmable water bath (Grant GP200, UK). To keep track of the mussel body temperature, thermocouples were also inserted into two mussels that served as dummies before being placed in the water bath. Gill temperatures were recorded by thermocouples (Omega K-type, Teflon insulated, tip diameter 0.25mm) inserted between the valves and connected to a portal digital thermometer. The water bath temperature was programmed to raise the mussel body temperature from  $27^\circ\text{C}$  to  $40^\circ\text{C}$  at different warming rates (Figure 4).

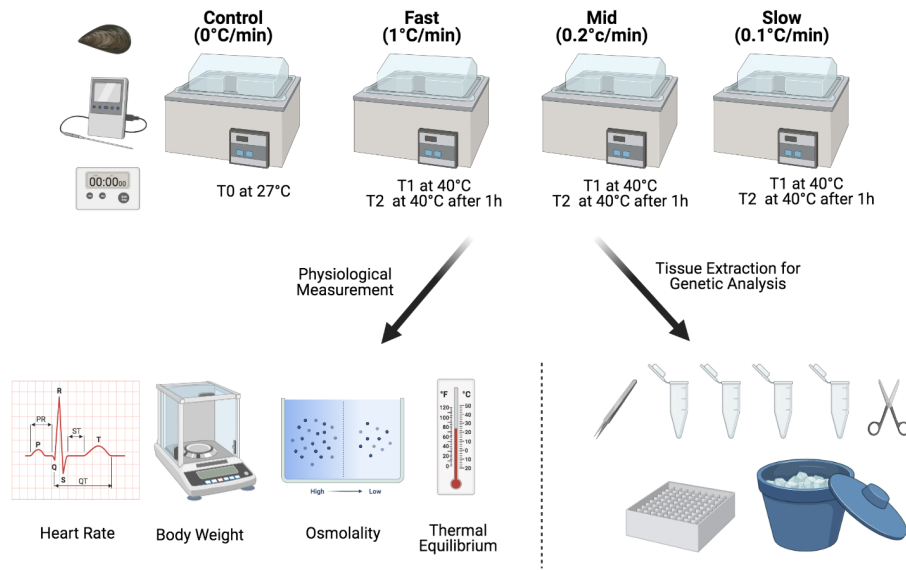


Figure 4. *Diagram showing experimental workflow of taking physiological measurements and extracting tissue for downstream genetic analysis during warming experiments*

Previous trial runs show that there is a lag in mussel body temperature compared to the surrounding water bath temperature and this relationship also changes with different warming rates. To account for that, the maximum water bath temperatures for each warming rate were adjusted so that the final body temperature of the mussels consistently reached  $40^\circ\text{C}$  across the three different warming rates ( $55^\circ\text{C}$  for fast,  $46^\circ\text{C}$  for mid,  $44.5^\circ\text{C}$  for slow). The animals were placed into ambient air-filled vials in the water bath at  $28^\circ\text{C}$  for 10 minutes before the water bath temperature started ramping up. The body temperatures of the mussel dummies were closely monitored to prevent the animals from reaching the Arrhenius Breakpoint Temperature (ABT), which is around  $41^\circ\text{C}$  in air for *M. virgatus* (Williams, unpublished data). Upon reaching  $40^\circ\text{C}$ , animals were immediately transported to a water bath kept at  $42^\circ\text{C}$  to maintain their body temperature at  $40^\circ\text{C}$  for another hour. Various physiological measurements and tissue extraction were performed at three time points: 10 minutes after animals were placed into the water bath (T0: preheating), when the animals first reached  $40^\circ\text{C}$  (T1: after heating), an hour acclimation after reaching  $40^\circ\text{C}$  (T2: acclimation).

## 2.3 Physiological Measurements

The physiological responses measured were heart rate, osmolality of mantle water and thermal equilibrium (including mean and standard deviation of body temperature) as a proxy for metabolic rate, evaporative water loss and thermal response. Heart rates (Hz, beats s<sup>-1</sup>) were monitored for 10 minutes using infrared sensors (Vishay Semiconductors, CNY70, USA) attached to mussel shells near the heart at the mid-dorsal posterior hinge with Blue-Tac and connected to a PowerLab via an amplifier to a PowerLab (8/30 ADinstruments, Germany). Heart rates were manually counted by importing the files from PicoScope 4000A Series oscilloscopes to the software. To calculate the frequencies, the number of peaks was divided by the time period, averaged across the recorded measurements. Mantle water was collected by inserting a 10mm diameter filter paper disc (Wescor Inc., Logan, UT, USA) between the foot and mantle to determine osmolality using a vapour pressure osmometer (Wescor 5520, Wescor Inc.). A thermograph was taken of the mussel body by a thermal camera when the final temperature of 40°C is reached. The average and standard deviation of the mussel body temperature were determined using the Testo IRSoft Thermography Analysis Software. Three-way analysis of variance (ANOVA) was performed to investigate the differences in the physiological indicators within and between treatments. Levene's test was used to test for homogeneity of variances. Where there are significant differences, Tukey's HSD test was used to compare the means across groups. All statistical analyses were performed with R software (Version 4.0.2. R Core Team, 2020).

## 2.4 Genetic Measurements

At each time point (T0, T1 and T2), 4 mussels per control and treatment group were killed for gene expression analysis, with gill tissues frozen in liquid nitrogen and stored at -80°C until further processing. Total RNA was extracted from the mussel gill tissue using the commercial kit E.Z.N.A. Mollusc RNA (Omega Biotek) and quantified with a NanoDrop Spectrophotometer (ND-1000, Wilmington, DE, USA) and an Invitrogen Qubit Fluorometer (Thermo Fisher Scientific, USA). 2 RNA samples with RNA Integrity Number (RIN) > 8.0 per control group and 3 samples per treatment group determined by an Agilent 2100 Bioanalyzer (Agilent Technologies, California, USA) were sent to Novogene Co., Ltd (Beijing, China) for cDNA library construction and Illumina sequencing.

To perform de novo transcriptome assembly, failed reads from FASTQ files were removed using CASAVA version 1.8.2. The raw reads were pooled for pre-processing and assembly by trimming adaptors and filtering reads with more than 5% ambiguous bases, 50% bases with quality value < 10 or reads length < 40bp. The resulting high-quality reads were used for de novo

transcriptome in Trinity (version r2002-10-25; Grabherr et al., 2011) with k-mer length set at 25. Full-length transcripts assembly and spliced isoforms were clustered using CD-HIT v4.5.4 with a similar score > 95% (Li and Godzik, 2006) to classify the longest transcript from each sequence cluster as a functional gene unit.

All assembled non-redundant transcripts > 200bp were annotated using the NCBI nr and molluscan EST (expressed sequence tags) databases. They were submitted to Blast2GO (Conesa et al., 2005) to be assigned with GO terms for functional annotation. The abundance and expression level of each transcript were estimated using RSEM (verion1.2.3; Li and Dewey, 2011) based on FPKM (fragments per kilobase per million reads). Differential gene expression analysis was performed using DESEQ2 and EdgeR to visualize the gene expression patterns in the treatment groups with annotated functional pathways (Figure 5).

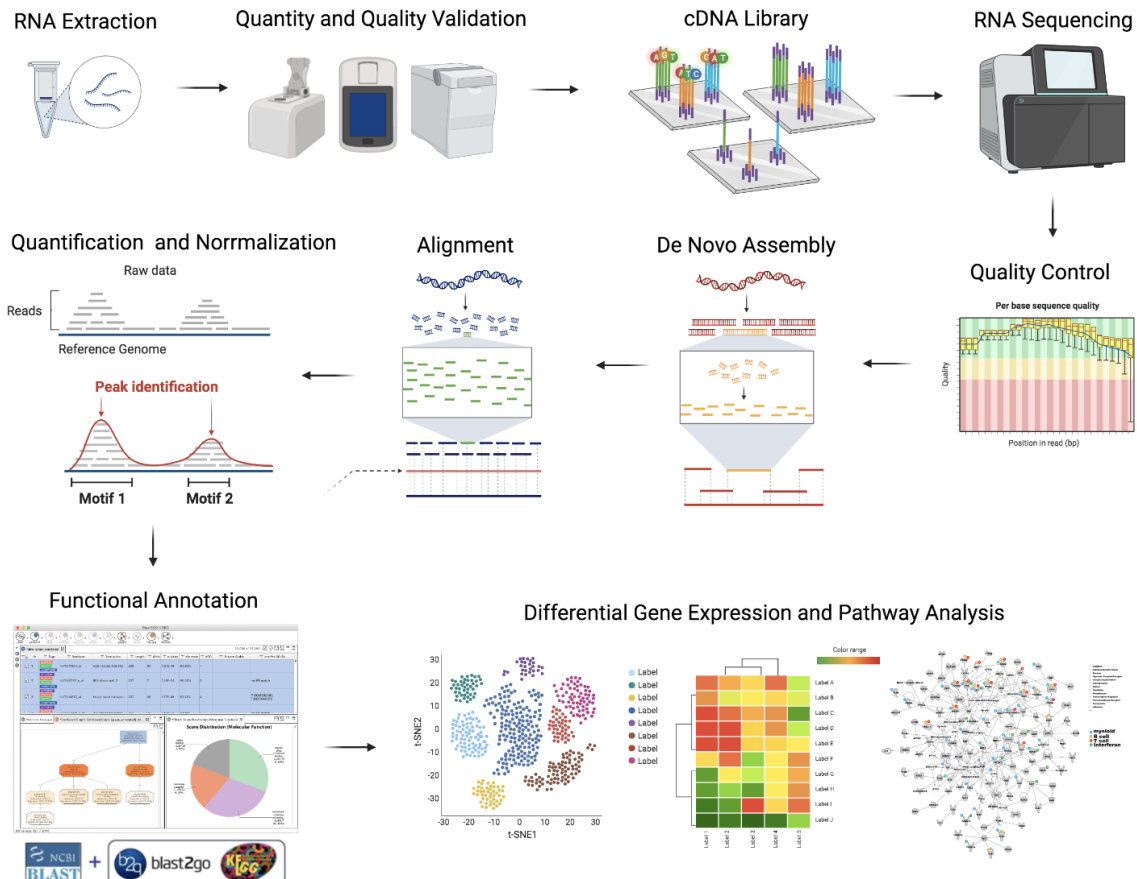


Figure 5. RNA sequencing and gene expression analysis pipeline

### 3. RESULTS

#### 3.1 Physiological Analysis

The responses of the mussels were compared across three warming rates between the two shore populations for rapid stress response after heating (T1) and acclimation response (T2). Due to measurement difficulties, the number of replicates for each treatment and time point differed between physiological variables and is listed in Table S1. To control for the effects of potential confounding covariates, a correlation matrix was computed (Figure 6). None of physiological traits were dependent on morphological traits such as body weight or shell length, but shell length was found to be positively correlated with average weight ( $R^2 = 0.441$ ,  $p < 0.05$ ). Later analysis was focused on using average weight as a proxy of size and mass of animal.

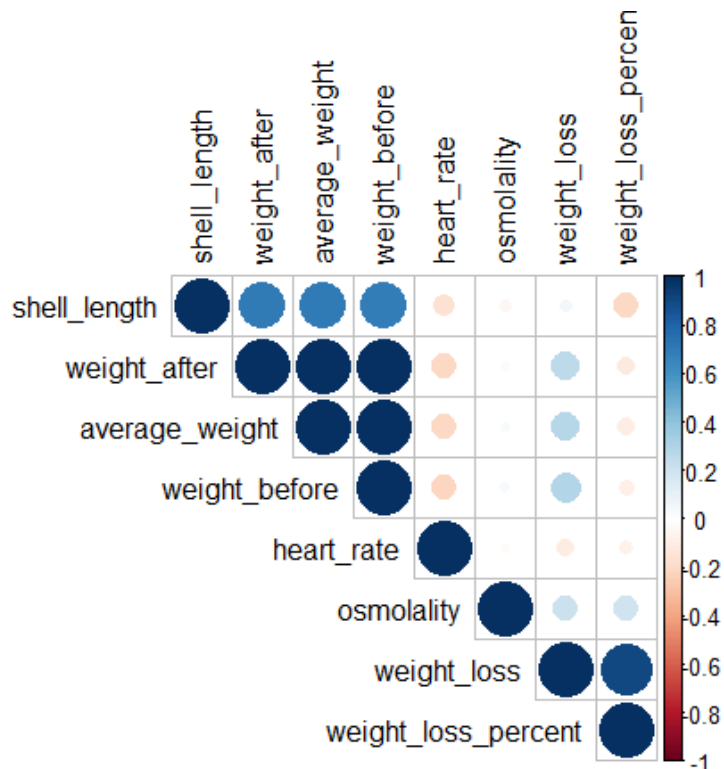


Figure 6. Correlation Matrix of Physiological Variables ( $p < 0.05$ ). Size of circles indicates the number of individual observations with correlation while the color on y-scale indicates the magnitude of correlation.

Amongst the four physiological indicators, the only significant differences found between treatments were for heart rate, weight loss percentage and average body temperature. Time point ( $p = 0.013$ ) significantly affected the heart rates of *M. virgatus*, with heart rates after heating significantly higher than after acclimation (Figure 7). The average heart rate in water at 27°C

(around 0.46Hz in the high-shore population and around 0.25Hz) was significantly higher than that in air at 27°C. While heart rates in both populations at the three warming rates were generally higher than the control rates in air, the differences were not statistically significant.

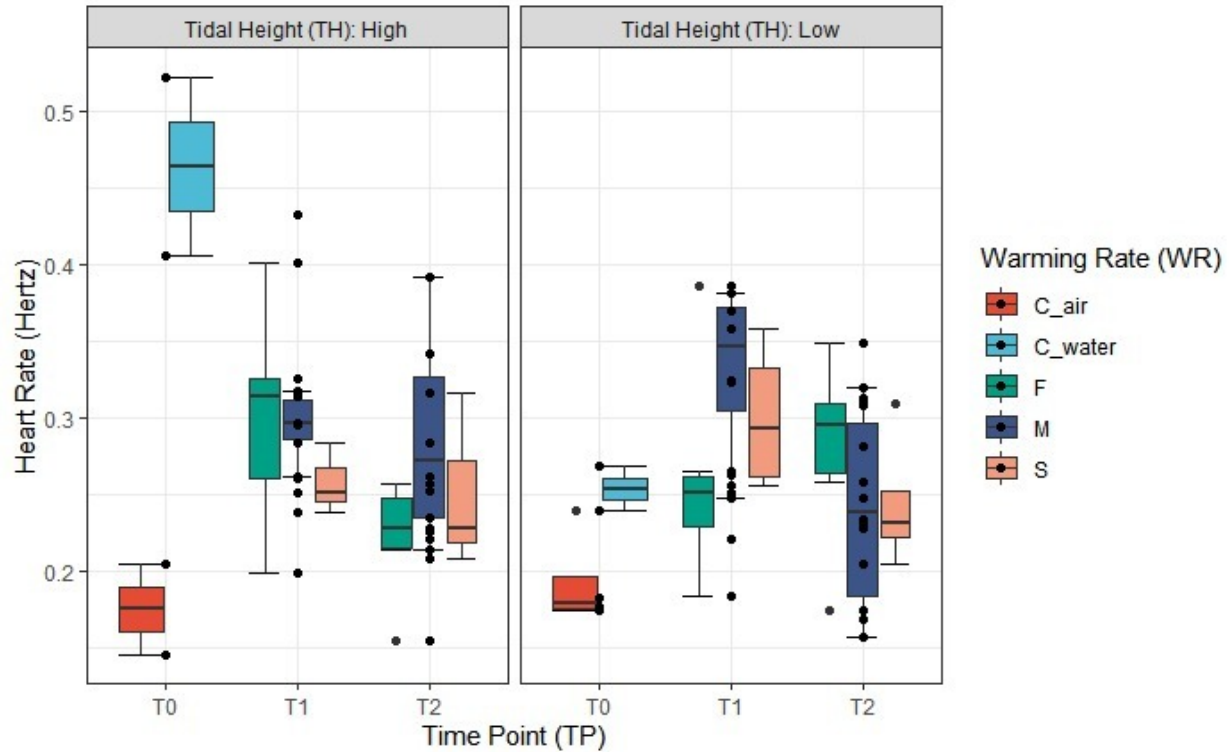


Figure 7. Box and whiskers plots to illustrate the median (mid-line), interquartile range (box) and 95% confidence intervals (error bars) of heart rate (hertz) of *M. virgatus* during pre-heating (T0), after heating (T1) and acclimation (T2) across fast (F), mid (M) and slow (S) warming rates in air at 40°C compared to controls in air (C\_air) and water (C\_water) at 27°C for high-shore (left) and low-shore (right) populations. Dots represent individual samples from the time point across rates.

Table 1. Three-way analysis of variance (ANOVA) to investigate the differences in heart rates of *M. virgatus* under three different warming rates (fixed factors: fast, mid, slow) at two time points (fixed factors: after heating T1 and acclimation T2) between two shore populations (high and low). Variances were homogeneous (Levene's test,  $p < 0.05$ ).

	Df	Sum Sq	Mean Sq	F value	Pr(>F)
heating_rate	2	0.0087	0.0044	1.21	0.31
tidal_height	1	0	0	0	0.99
time_point	1	0.024	0.024	6.66	0.013 *
heating_rate x tidal_height	2	0.0041	0.0021	0.57	0.57
heating_rate x time_point	2	0.0026	0.0013	0.36	0.69
tidal_height x time_point	1	0.00005	0.000048	0.013	0.91
heating_rate x tidal_height x time_point	2	0.021	0.011	2.91	0.064 .
Residuals	47	0.17	0.0036		

No statistically significant differences were found between treatment groups varying in warming rate, tidal height and time point in the osmolality levels of *M. virgatus*. Large spread of the data was observed across groups (Figure 8).

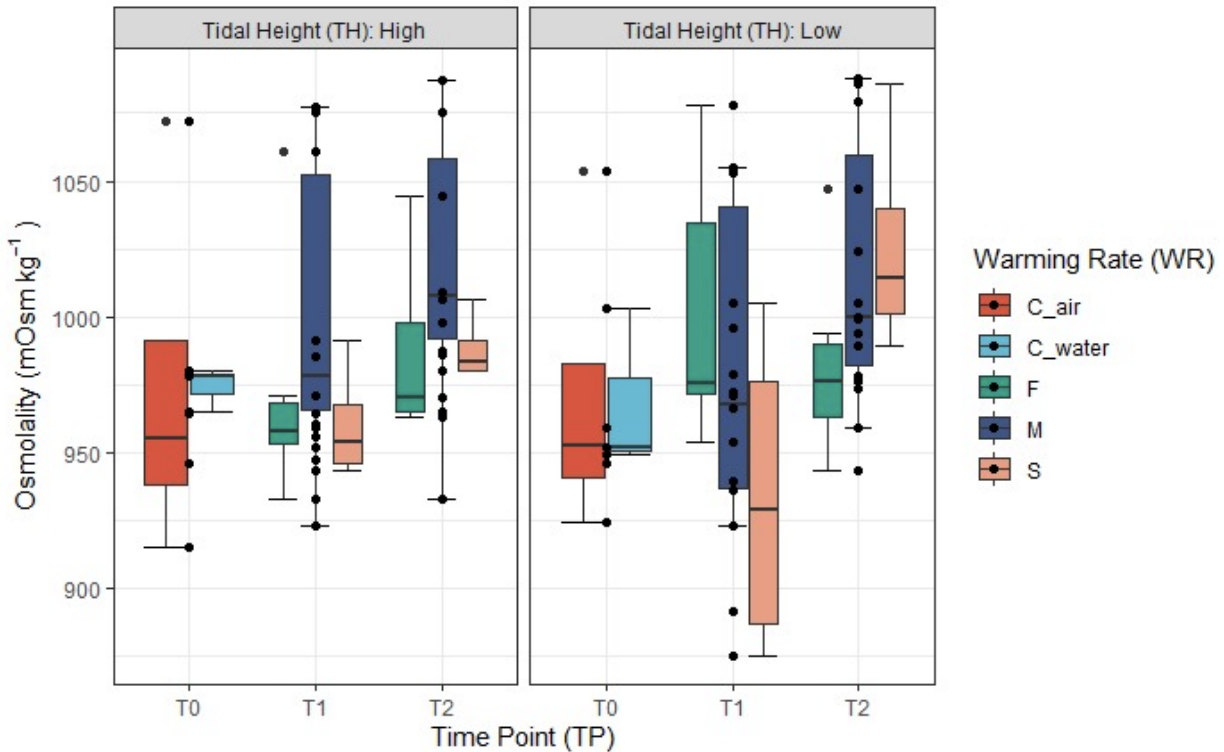


Figure 8. Box and whiskers plots to illustrate the median (mid-line), interquartile range (box) and 95% confidence intervals (error bars) of osmolality ( $\text{mOsm kg}^{-1}$ ) of *M. virgatus* during pre-heating (T0), after heating (T1) and acclimation (T2) across fast (F), mid (M) and slow (S) warming rates in air at  $40^\circ\text{C}$  compared to controls in air (C\_air) and water (C\_water) at  $27^\circ\text{C}$ .

for high-shore (left) and low-shore (right) populations. Dots represent individual samples from the time point across rates.

Table 2. Three-way analysis of variance (ANOVA) to investigate the differences in osmolality ( $mOsm\ kg^{-1}$ ) of *M. virgatus* under three different warming rates (fixed factors: fast, mid, slow) at two time points (fixed factors: after heating T1 and acclimation T2) between two shore populations (high and low). Variances were homogeneous (Levene's test,  $p < 0.05$ ).

	Df	Sum Sq	Mean Sq	F value	Pr(>F)
heating_rate	2	7766	3883	1.62	0.21
tidal_height	1	173	173	0.072	0.78
time_point	1	9134	9134	3.81	0.057
heating_rate x tidal_height	2	1070	535	0.22	0.81
heating_rate x time_point	2	9007	4503	1.88	0.16
tidal_height x time_point	1	361	361	0.15	0.69
heating_rate x tidal_height x time_point	2	5866	2933	1.22	0.30
Residuals	51	122337	2399		

There was a general increasing trend in the percentage of weight loss with slower warming rates and over longer time periods ( $p = 0.0012$  and  $p = 0.00024$  respectively) (Figure 9). While all three warming rates had significantly higher weight loss percentages than the control rate in air (except fast) and water, weight loss percentage only significantly increased between fast and mid as well as fast and slow rates, but not between mid and slow rates (Table 3).

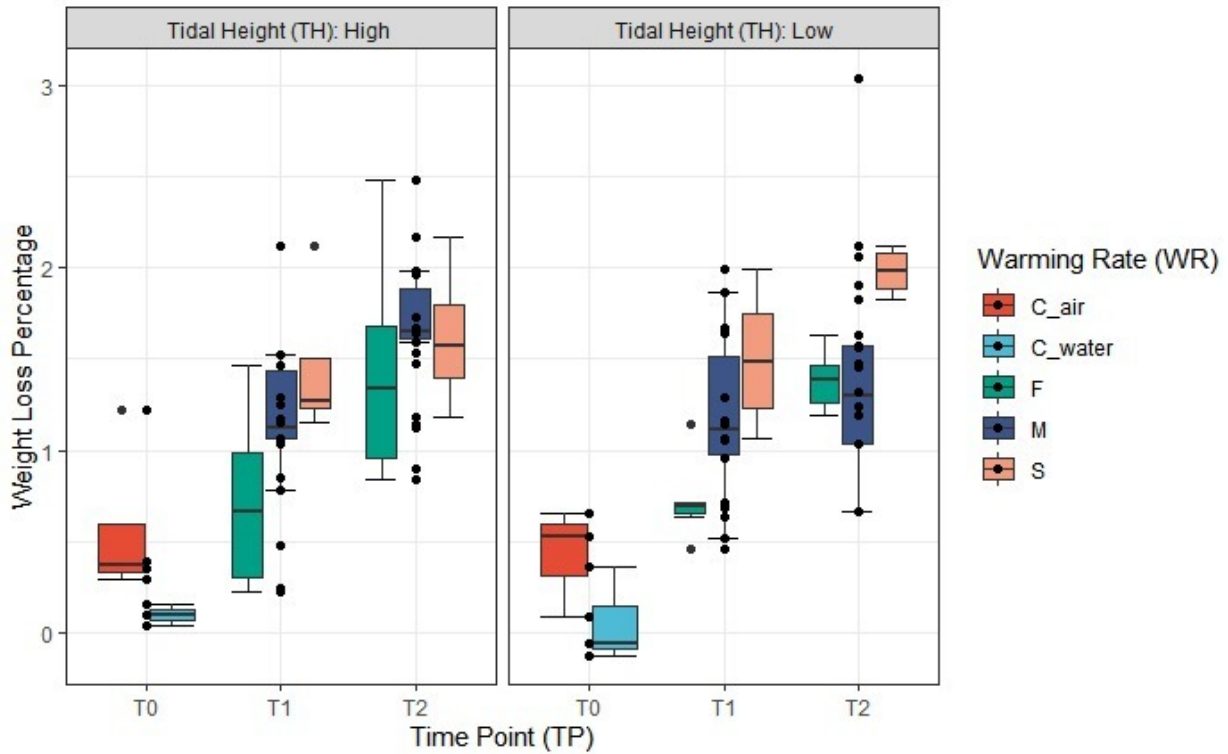


Figure 9. Box and whiskers plots to illustrate the median (mid-line), interquartile range (box) and 95% confidence intervals (error bars) of weight loss percentage of *M. virgatus* during pre-heating (T0), after heating (T1) and acclimation (T2) across fast (F), mid (M) and slow (S) warming rates in air at 40°C compared to controls in air (C\_air) and water (C\_water) at 27°C for high-shore (left) and low-shore (right) populations. Dots represent individual samples from the time point across rates.

Table 3. Three-way analysis of variance (ANOVA) to investigate the differences in weight loss percentage of *M. virgatus* under three different warming rates (fixed factors: fast, mid, slow) at two time points (fixed factors: after heating T1 and acclimation T2) between two shore populations (high and low). Variances were homogeneous (Levene's test,  $p < 0.05$ ). Post-hoc Tukey tests were used to further separate significant factors.

	Df	Sum Sq	Mean Sq	F value	Pr(>F)
heating_rate	2	3.36	1.68	7.65	0.0012 **
tidal_height	1	0.001	0.001	0.004	0.95
time_point	1	3.42	3.42	15.57	0.00024 ***
heating_rate x tidal_height	2	0.27	0.14	0.62	0.54
heating_rate x time_point	2	0.49	0.25	1.12	0.33
tidal_height x time_point	1	0.002	0.002	0.009	0.93
heating_rate x tidal_height x time_point	2	0.11	0.055	0.25	0.78
Residuals	52	11.43	0.22		

The average body temperatures stayed relatively constant at around 27°C in both control groups when taken out of the water bath while the treatment groups decreased by different amounts from 40°C when the measurements were taken at room temperature (Figure 10). The slow rate had a significantly higher body temperature than both the fast and mid rates but the latter two shared similar measurements (Table 4). The average body temperature after heating (T1) was also significantly lower than acclimation (T2) but was not different between high-shore and low-shore populations.

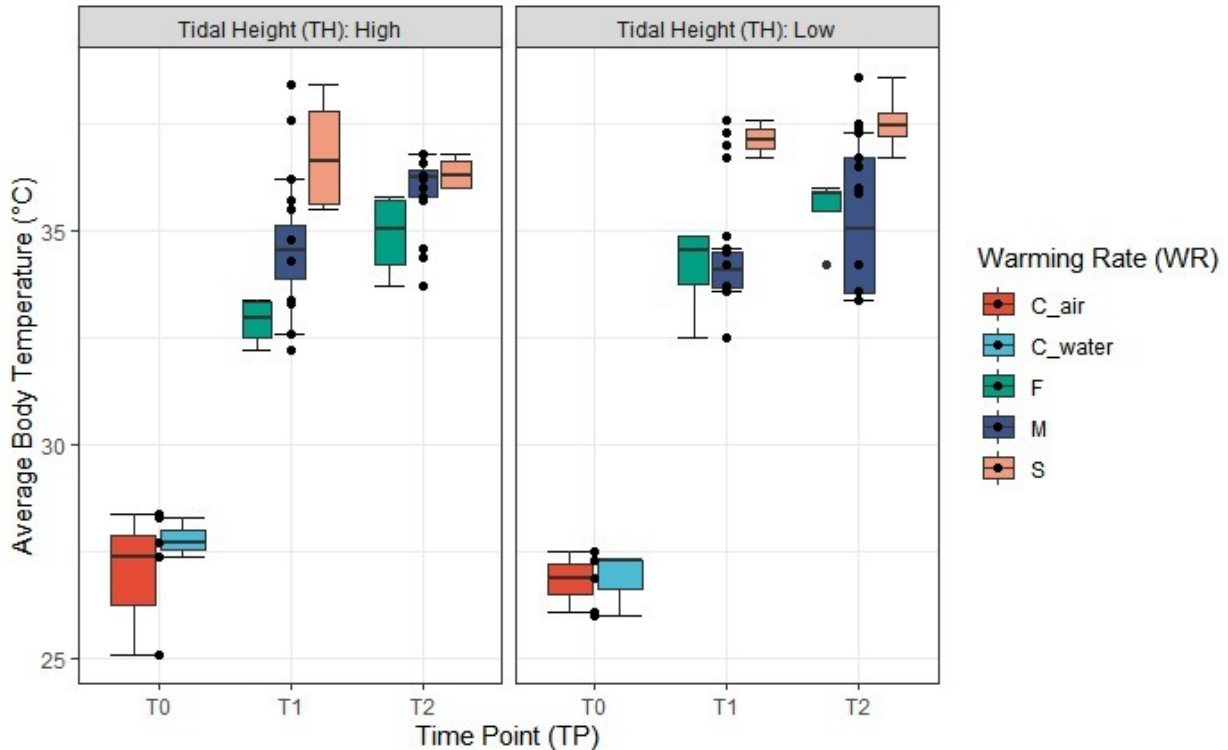


Figure 10. Box and whiskers plots to illustrate the median (mid-line), interquartile range (box) and 95% confidence intervals (error bars) of average body temperature (°C,  $n = 4$ ) of *M. virgatus* during pre-heating (T0), after heating (T1) and acclimation (T2) across fast (F), mid (M) and slow (S) warming rates in air at 40°C compared to controls in air (C\_air) and water (C\_water) at 27°C for high-shore (left) and low-shore (right) populations. Dots represent individual samples from the time point across rates.

Table 4. Three-way analysis of variance (ANOVA) to investigate the differences in average body temperature of *M. virgatus* under three different warming rates (fixed factors: fast, mid, slow) at two time points (fixed factors: after heating T1 and acclimation T2) between two shore populations (high and low). Variances were homogeneous (Levene's test,  $p < 0.05$ ). Post-hoc Tukey tests were used to further separate significant factors.

	Df	Sum Sq	Mean Sq	F value	Pr(>F)
--	----	--------	---------	---------	--------

heating_rate	2	60.11	30.06	26.25	9.3e-08 ***
tidal_height	1	1.69	1.69	1.47	0.23
time_point	1	11.8	11.80	10.31	0.0028 ***
heating_rate x tidal_height	2	5.46	2.73	2.38	0.11
heating_rate x time_point	2	6.52	3.26	2.85	0.071 .
tidal_height x time_point	1	0.01	0.013	0.012	0.91
heating_rate x tidal_height x time_point	2	1.29	0.65	0.56	0.57
Residuals	36	41.22	1.15		

## 3.2 Genetic Analysis

### 3.2.1 De Novo Assembly

A total of 849,200 sequences were generated from total RNA extractions of 5 pooled *M. virgatus* samples across both control and treatment groups with a mixture of high and low-shore individuals after heating and acclimation. The number of raw reads among samples ranged between 40.4 and 57.4 million (mean = 46.5 million, SD = 3.3 million), showing similar quality scores (mean Q-scores  $\geq 30 = 93.0\%$ , Table S2). Given the contigs were highly redundant, they were carefully filtered at 90% identity to reduce complexity, resulting in 495,236 gene clusters. Only 64,453 transcripts were found to have functional roles according to coding sequences. 97.25% of the BUSCO groups had complete gene representation (single-copy or duplicated), while 1.96% were only partially recovered, and 0.78% were missing. Quality metrics of the assembled transcriptome at the three stages of assembly, clustering and coding were summarized in Table 5. All downstream analyses were performed based on de novo reference transcriptome.

Table 5. Summary statistics of de novo assembled transcriptome of *M. virgatus*. The de novo assembly was filtered to gene clusters and subsequently annotated for coding sequences.

	Assembly	Clustering	Coding
Total number of transcripts	849,200	495,236	64,453
Number of transcripts (>500 bp)	333,700	165,525	12,420
Number of transcripts (>1000 bp)	15,091	66,365	3,375
Average assembled length	753.591	641.283	353.089
Maximum length	33,899	33,899	9,706
N50	1,225	874	502
BUSCO completeness (%)	98.82	98.43	97.25
BUSCO fragmented (%)	0.0	0.39	1.96
BUSCO missing (%)	1.18	1.18	0.78

### 3.2.2 Functional Annotation

Out of the 64,453 tentative consensus sequences with an N50 (the length of contig that makes up 50% of the total assembly length) of 502bp, >90% were annotated using InterPro database, ~79% were blasted to known proteins in public databases such as NCBI and UniProt while ~2% had no matches which might represent unknown function or low similarity to published sequences (Figure 11). A majority of the annotated transcripts had significant alignment with the Bivalvia class, including the Pacific oyster *Crassostrea gigas* (~13.8%), followed by the Great scallop *Pecten maximus* (~13.7%), the Japanese scallop *Mizuhopecten yessoensis* (~13.2%), the Eastern oyster *Crassostrea virginica* (~10.2%) and the Mediterranean mussel *Mytilus galloprovincialis* (~8.9%, Figure 12).

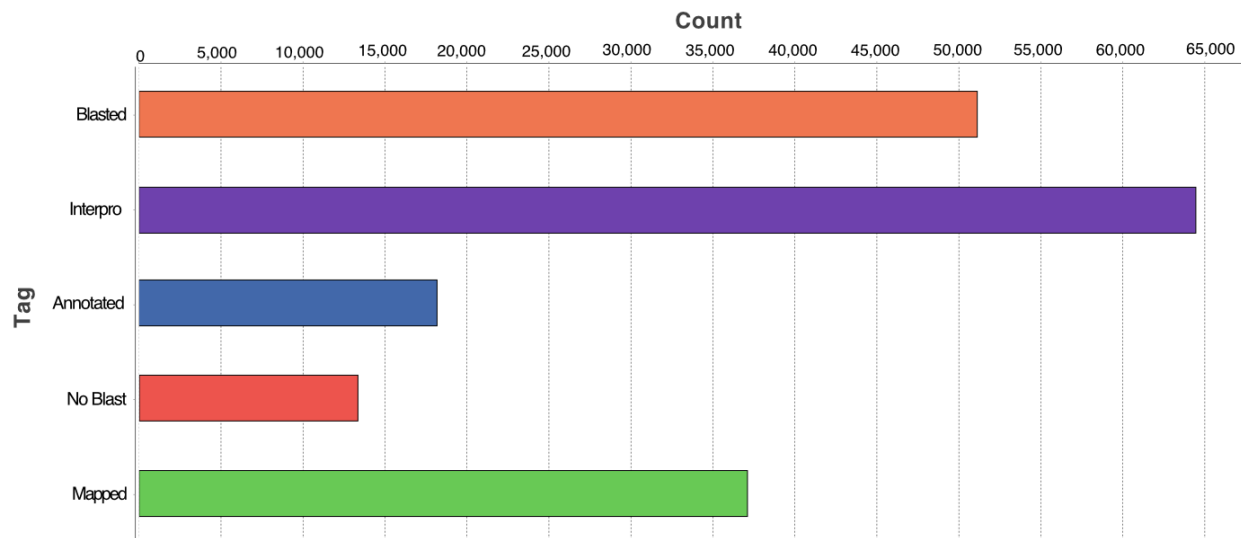


Figure 11. Tag distribution of potential transcripts against public databases

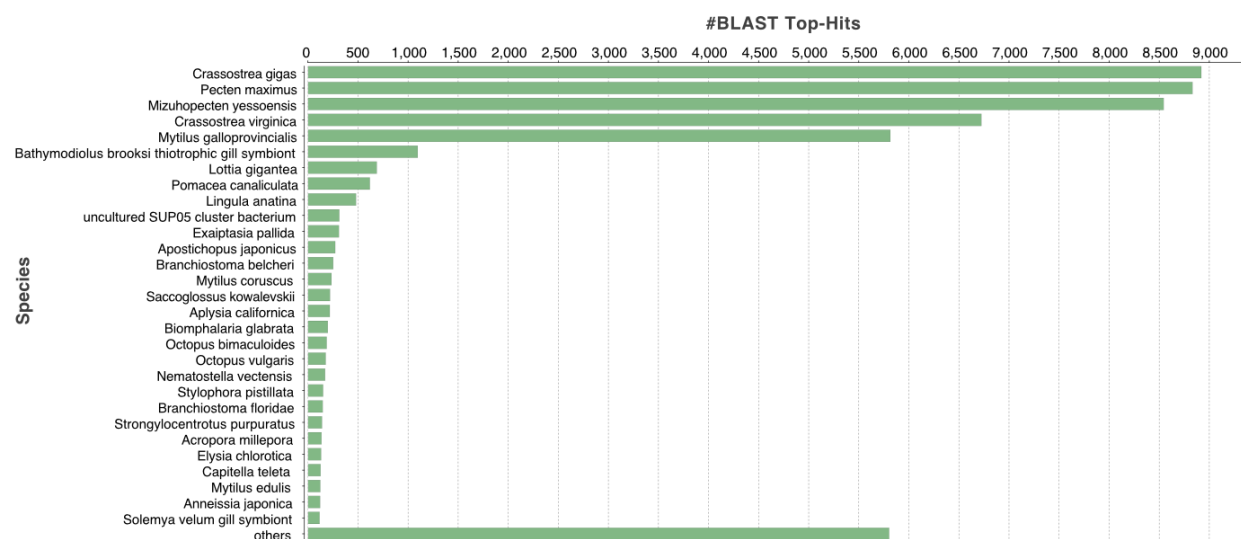


Figure 12. *Distribution of annotated transcripts against known species sequences in public databases*

The potential functions of the blasted transcripts were uncovered through gene ontology (GO) annotations from Blast2Go, InterProScan and KEGG Orthology databases. The GO annotations were distributed among the categories with a higher representation of molecular functions (MF, 20.0%), followed by biological processes (BP, 17.2%) and cellular components (CC, 16.7%). Molecular functions describe the activities, such as catalysis or binding, performed by a gene product at a molecular level, while biological processes refer to larger processes occurring on the cellular or organismal level that are accomplished by multiple gene products. Cellular components, on the other hand, indicate the location of a cellular structure where a gene product performs its function. In molecular function, most of the GO terms were grouped into binding and catalytic activity (Figure 13, Figure S5). In biological processes, cellular process, metabolic process and biological regulation were the major activities (Figure 13, Figure S6). In cellular components, the highest percentage of GO terms was associated with the membrane, followed by cell and organelle (Figure 13, Figure S7).

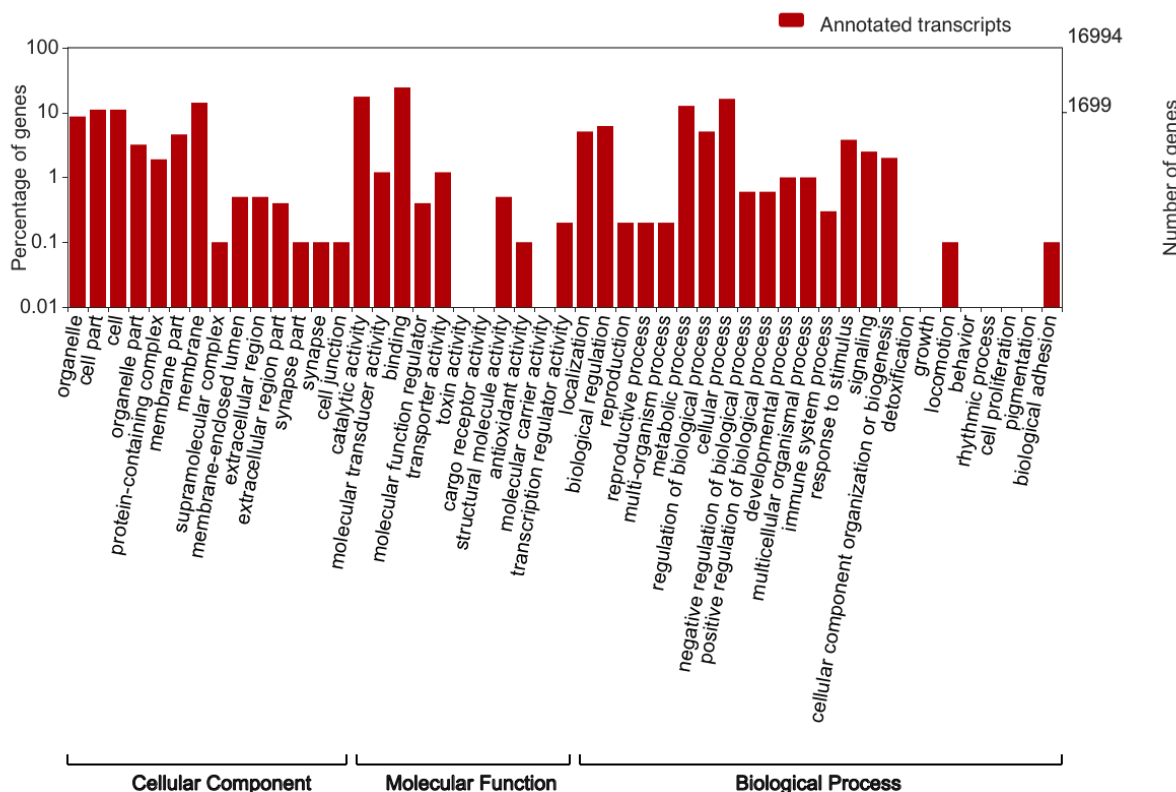


Figure 13. *Distribution of transcripts in GO terms in cellular component, molecular function and biological process*

### 3.2.3 Differential Gene Expression

During the first transition from water to air, of the 64,453 annotated transcripts, only 235 genes were significantly regulated ( $p\text{-adjusted} < 0.05$  and absolute log fold change  $> 1.5$ ). A total of 102 genes were downregulated and 133 upregulated. Figure 14 shows the top 15 upregulated and downregulated genes. Amongst the top downregulated genes with the highest fold change ( $> 10$ ) were SL9A2 (sodium-hydrogen exchanger involved in pH regulation), BRPF1 (histone acetylation in gene regulation), PEPD (collagen metabolism) and LZTR1 (protein ubiquitination). Conversely, upregulated genes with over 10-fold log change included SSH2 (protein phosphatase), SPTCB (spectrin for maintenance of plasma membrane integrity and cytoskeletal structure), KLC (kinesin light chain in microtubule transport), UBC9 (ubiquitin conjugating enzyme) and SYFB (phenylalanine-tRNA ligase) (Figure 14).

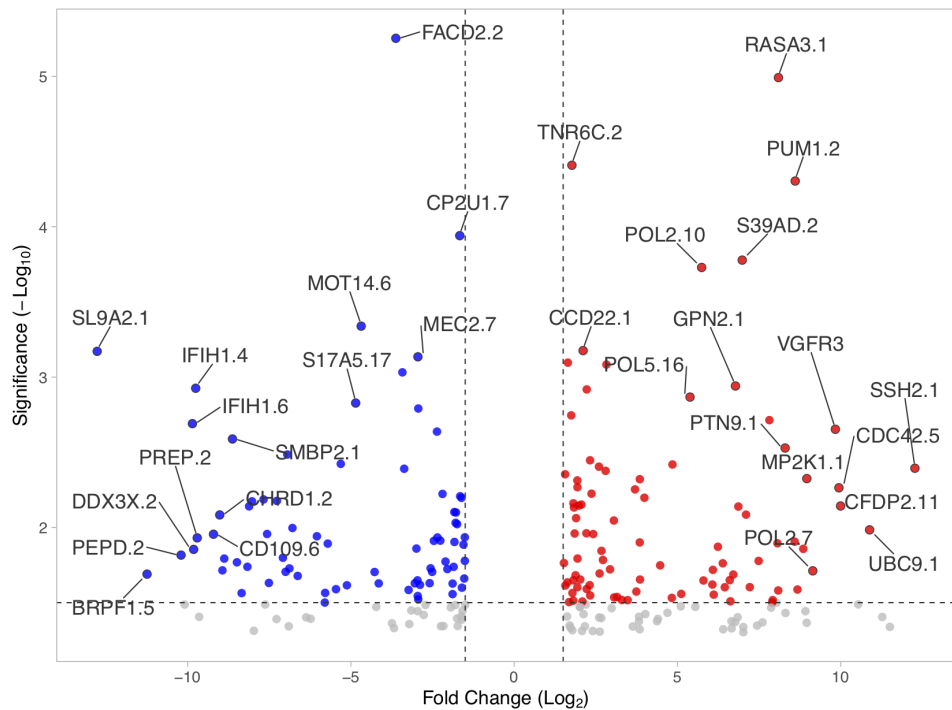


Figure 14. Top 15 upregulated and downregulated genes of control mussels moving from water to air. Red dots represent significantly upregulated genes with log fold change  $> 1.5$  and  $p\text{-value adjusted} < 0.05$  while blue dots represent significantly downregulated genes with log fold change  $< -1.5$  and  $p\text{-value adjusted} < 0.05$ .

All activities within the molecular functions involved both down and upregulated genes, whereas a few cellular components and biological processes indicated only upregulated or downregulated genes during air exposure. Upregulation occurred at cell division sites and membranes of organelles and mitochondria whereas only endoplasmic reticulum membranes were associated with downregulated genes. Moreover, biological processes related to stress response, such as cell death, cell communication, signal transduction, immune response, response to stimulus and

catabolic process were upregulated only while glycosylation, biosynthetic process and system process were downregulated (Figure 15).

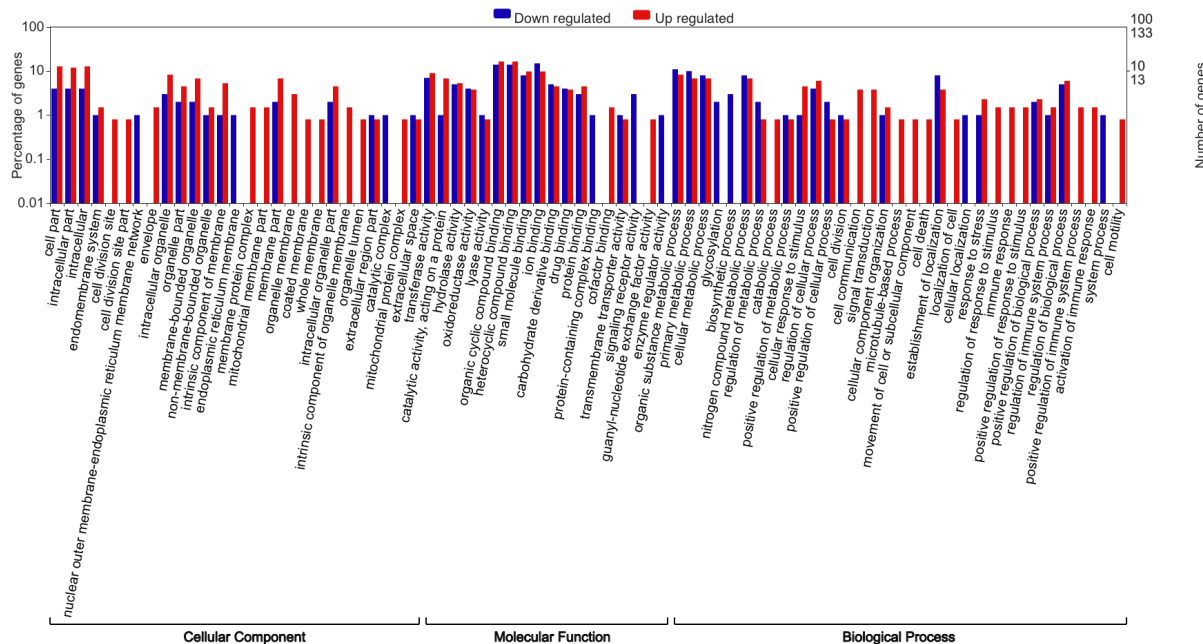


Figure 15. *GO terms of down and upregulated genes in mussel transition from water to air that are categorized into cellular component, molecular function and biological process. Both percentage and number of genes significantly downregulated (blue) and upregulated (red) are indicated ( $p$ -value adjusted  $< 0.05$ ).*

Among the upregulated biological processes, majority of the enriched functional pathways fell under macromolecular metabolic process, phosphorylation and regulation of apoptotic process amongst a few others (as indicated by the plot size as a proxy of the number of transcripts with the particular GO term association) (Figure 16).

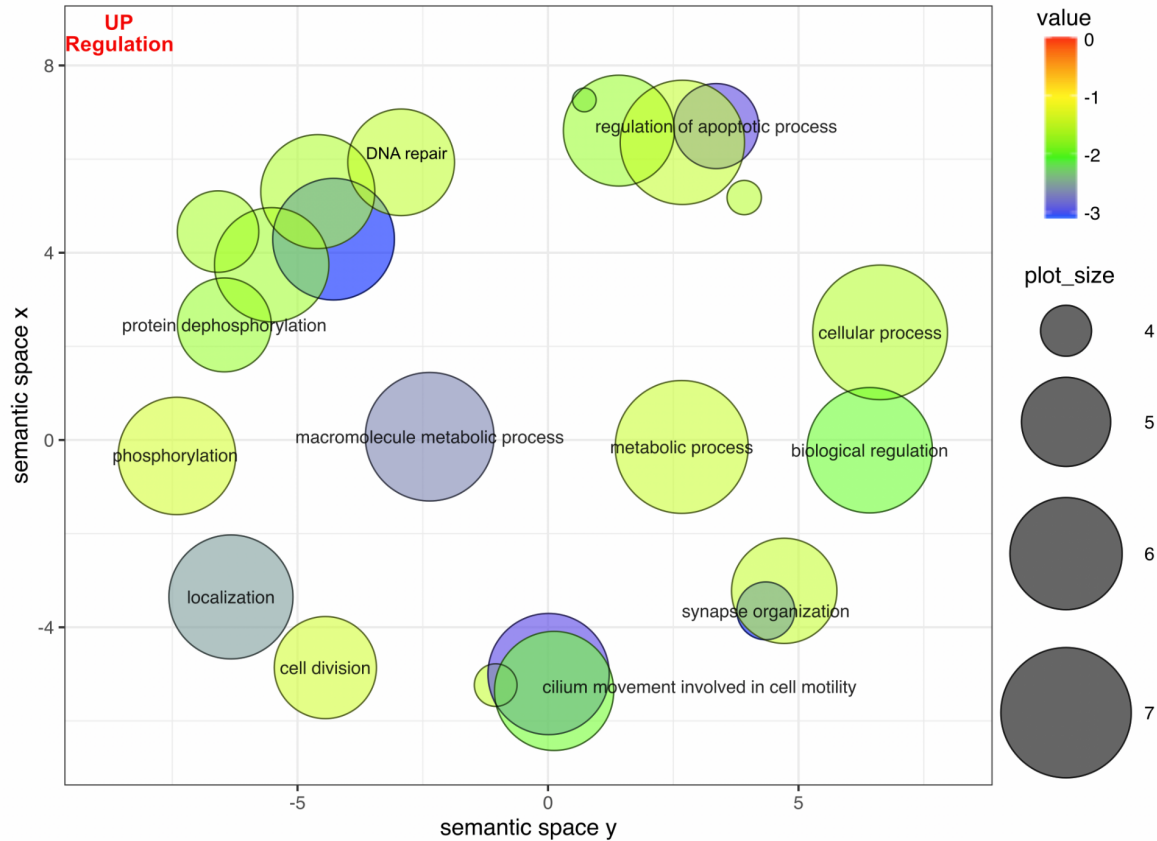


Figure 16. GO Enrichment analysis of the types of pathways with upregulated genes in control mussels moving from water to air. Value with color legend represents the p-value significance of enrichment and plot size indicates the number of transcripts that fall under the functional pathway.

In contrast, while DNA repair, cell division and synapse organization were common pathways with both upregulated and downregulated genes, phosphorylation of RNA polymerase II C-terminal domain, inorganic anion transport, glycosylation and other metabolic processes (including carbohydrate, lipid and cellular aldehyde) were significantly downregulated as mussels transition from water to air medium (Figure 17).

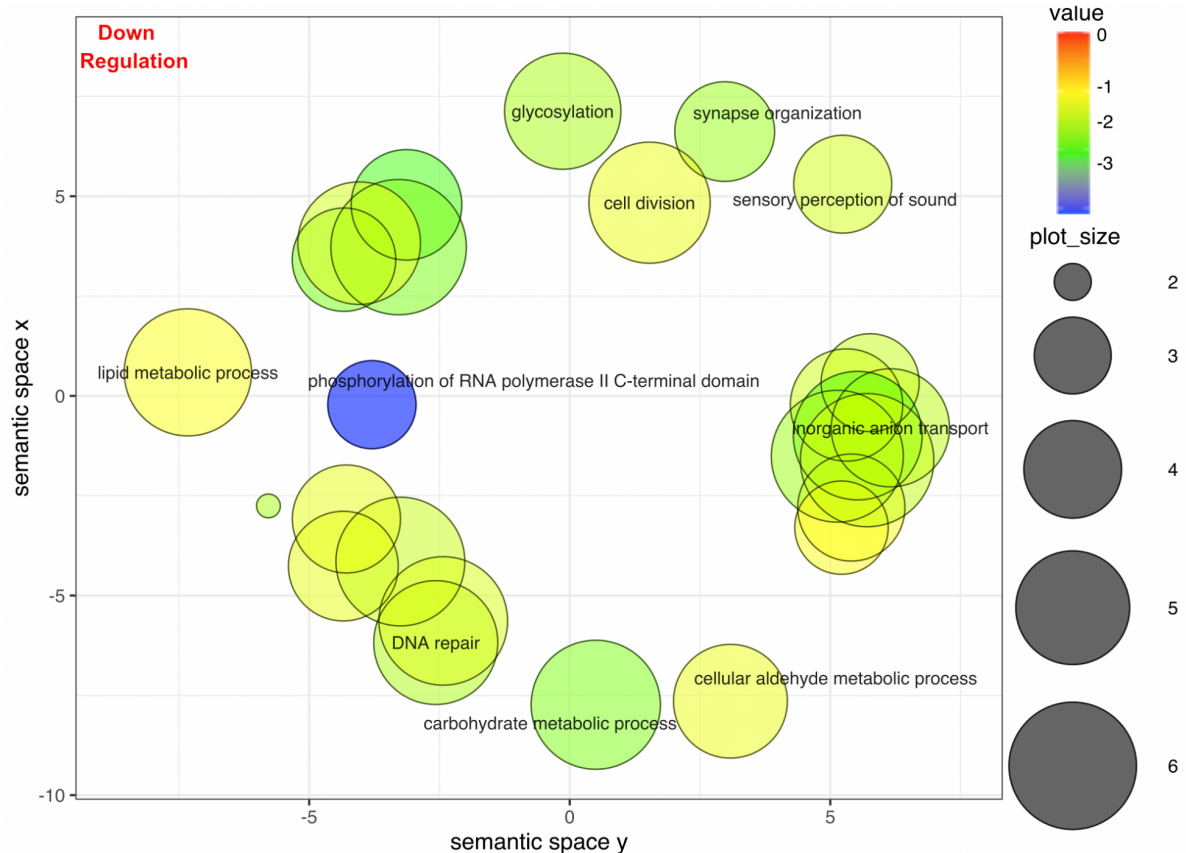


Figure 17. GO Enrichment analysis of the types of pathways with downregulated genes in control mussels moving from water to air. Value with color legend represents the p-value significance of enrichment and plot size indicates the number of transcripts that fall under the functional pathway.

During the transition from air at 27°C to 40°C at different warming rates, for the fast rate, the high shore population had 71 upregulated genes ( $p\text{-value} < 0.01$  and absolute log fold change  $> 1.5$ ) and 51 downregulated genes whereas the low shore population had 60 upregulated and 46 downregulated genes. For the mid rate, the high shore population had 60 upregulated and 36 downregulated genes whereas the low shore population had 75 upregulated and 48 downregulated genes. For the slow rate, the high shore population had 76 upregulated and 45 downregulated genes whereas the low shore population had 104 upregulated and 112 downregulated genes (Table 6). Amongst all significant genes, HSP71 (heat shock protein) was the only upregulated gene shared by both high and low shore populations across all three rates, except in low-shore population at the fast rate (Table S3). The high-shore population had the highest expression of HSP71 at the mid rate (13.19 log fold change), only  $<0.13$  log fold difference from the fast rate (13.06 log fold change), but the slow rate had more than a 1 log fold change difference (11.92 log fold change). The low-shore population, on the contrary, had

HSP71 most upregulated at the slow rate with 12.8-fold change, followed by 12.06-fold change at the mid rate.

During the rapid stress response, apart from HSP71, the three rates showed different transcriptional profiles of gene expression (Figure 18). Of the 60 genes based on the top 5 upregulated and downregulated genes in each shore population at each rate, there were only 41 unique genes, where 13 were upregulated and 28 downregulated (Figure 18). Many of the upregulated genes were shared across more than one rate and usually fell under protein folding (e.g. BIP and DNJB1), cell binding (e.g. CO6A5 and RADI), histone acetylation (e.g. MS3L1, EFCB6) and apoptosis inhibition (e.g. PIAP, PTC1 and TIF1A). Only C1QT3 (negative regulation of inflammatory response) and EFCB6 (calcium binding) were upregulated at the fast rate, but not mid or slow. Only one of the downregulated genes, FIBA (immune response), was shared between fast and slow rates while LZTR1 (cell growth, division and differentiation) was commonly expressed between the two shore populations at mid rate. Across all three rates, there was a set of genes that were only expressed in one of the two shore populations. In the high shore population, only SSH2 (protein phosphatase) was consistently expressed across all the rates, with decreasing expression at faster rates. In the low shore population, PIAP (putative inhibitor of apoptosis) showed increasing expression with faster rates whereas PTC1 (receptor for tumor suppressor) showed decreasing expression (Table S3).

When mussels were kept at 40°C for one-hour acclimation, for the fast rate, the high shore population showed 50 upregulated ( $p\text{-value} < 0.01$  and absolute log fold change  $> 1.5$ ) and 39 downregulated genes whereas the low shore population showed 36 upregulated and 61 downregulated genes. For the mid rate, the high shore population showed 48 upregulated and 44 downregulated genes whereas the low shore population showed 41 upregulated and 35 downregulated genes. For the slow rate, the high shore population showed 36 upregulated and 47 downregulated genes whereas the low shore population showed 47 upregulated and 61 downregulated genes (Table 6). Of the top genes regulated, the acclimation period resulted in a higher number of uniquely regulated genes as the rate decreased (Figure 18).

The transcriptional profile of both shore populations and across rates showed mostly different genes regulated during the acclimation response compared to the rapid stress response. Of the 56 regulated unique genes, 13 were shared across both responses within the same rate and shore population, 12 of which were downregulated during rapid stress response but upregulated during acclimation. While they were different genes being regulated, their opposite expression pattern was consistent across all rates and shore populations. These genes were DYHG (cell motility), IFIH1 (immune response), VWDE (signalling receptor binding) for the fast rate, JAK2 (immune response), LEO1 (transcriptional regulation), MS3L (transcriptional regulation) for the mid rate and BP10 (embryonic patterning), PREP (protein degradation), XIAP (apoptosis inhibition) for

the slow rate in the high population, and SL9A2 (pH regulation) for the mid rate and FICD (protein folding) for the slow rate in the low shore population.

No genes were shared across all three rates. Amongst the five genes shared between any two rates, four of them displayed a similar pattern of upregulation or downregulation across rates. ATLA (endoplasmic reticulum membrane biogenesis) was upregulated while MTSS1 (tumor suppression) and RMB4B (transcriptional regulation) were downregulated at both fast and mid rates. BRPF (histone acetylation) was downregulated at mid and slow rates. GIMA4 (apoptosis inhibition), however, was downregulated at the fast rate but upregulated at the slow rate. Of the upregulated genes, all rates had at least one immune-related gene (IFIH1 for fast rate, JAK2 for mid rate and FCN2 for slow rate). However, the slow rate further upregulated two genes that inhibit apoptosis (XIAP and GIMA4) whereas the fast rate upregulated GHITM that prompted mitochondrial apoptosis. Amongst the downregulated genes, all three rates shared genes that relate to transcriptional regulation (e.g. BRPF, C1D, MUT7, RBM4B, TADBP and PININ). The mid and slow rates also downregulated genes responsible for cell division (e.g. LAP2, TITIN, RAE1L) while the fast rate downregulated genes related to neuronal circuits and synaptic transmission (e.g. DLGP1, TADBP, RETR3 and PTPRT). The slow rate, on the contrary, downregulated genes that govern reactive oxygen species (ROS) generation (XDH) as well as protein degradation (NAS39) and folding (HS12A). Between the high and low shore populations, there were 4 genes shared but distributed between different rates. They were BRPF1 (histone acetylation), GIMA (apoptosis inhibitor), MTSS1 (tumor suppression) and RBM4B (transcriptional regulation).

*Table 6. Total number of significantly upregulated and downregulated genes between high and low shore populations at fast, mid and slow warming rates during the rapid stress (T0-T1) and acclimation (T1-T2) transitions*

	T0-T1 (Rapid Stress)				T1-T2 (Acclimation)			
	High Shore		Low Shore		High Shore		Low Shore	
	Up	Down	Up	Down	Up	Down	Up	Down
Fast	71	51	60	46	50	39	36	61
Mid	60	36	75	48	48	44	41	35
Slow	76	45	104	112	36	47	47	61

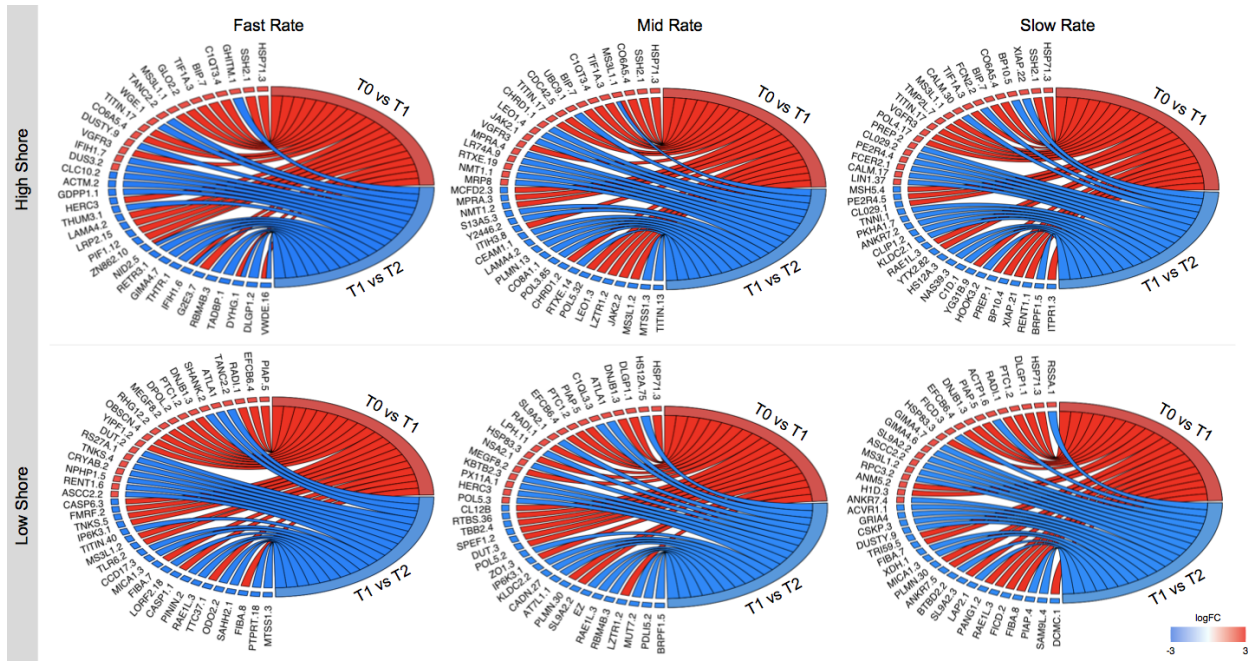


Figure 18. Circos plot showing the top upregulated and downregulated genes at different time points across the slow, mid and fast warming rates between high and low shore. Red represents significantly upregulated genes and blue represents significantly downregulated genes.

## 4. DISCUSSION

### 4.1 Transition from Water to Air

When mussels transition from submergence in seawater at high tide to emergence into aerial environment at low tide even at the same temperature, they face desiccation stress. This is reflected by higher water loss in control mussels at 27°C compared to their water counterparts at the same temperature. Despite previous research that suggests a positive correlation between evaporative water loss and osmotic balance (Segal and Dehnel, 1962; Wolcott, 1973), there is however no change in osmolality of the control animals despite weight loss. This may be explained by the experimental design where the control animals were only exposed to air for 20 minutes before measurement, enabling these animals to maintain osmotic homeostasis during short intervals despite abrupt changes in medium. While Newell (1979) concludes that the high shore population of a similar mussel species *Choromytilus meridionalis* better tolerates longer periods of desiccation than the low shore population, our results show that there are no statistical differences in the physiological responses of the control animals in air between high and low tides.

To cope with the new desiccation stress, these mussels are likely to enter a new physiological state and activate a variety of molecular mechanisms. This is reflected in the reduced heart rate in control animals in air as compared to their water counterparts. Heart rate has been positively linked with metabolic rate (Marshall and McQuaid, 1992) and a reduction in heart rate during emersion is considered a sign of metabolic depression (McMahon, 1988). As mussels are exposed to air, their reduced heart rate indicates slower metabolic rates. Consistent with previous research where more than 50 % in *Mytilus* species display slower heart rates in air than in water (Helm and Trueman, 1967; Coleman, 1973a; Bayne et al. 1976), a reduction in heart rate might be related to oxygen deficiency since mussels close their valves to limit oxygen consumption when emersed as a strategy to improve their thermal tolerance under hot temperatures (Widdows et al., 1979). This phenomenon of bradycardia (slow heart rates) is similarly observed in other marine ectotherms, such as *Mytilus californianus* (Bayne et al., 1976), *Patella vulgata* (Santini et al. 2000), *Echinolittorina malaccana* (Marshall et al. 2011), *Choromytilus meridionalis* and *Perna perna* (Marshall and McQuaid 1993).

Despite the lack of thermal change, the transition from water to air initiates a switch between aerobic and anaerobic metabolism, activating a repertoire of molecular responses and biochemical adjustments (Fan et al., 1991). The molecular changes observed in *M. virgatus* can be broadly categorized into four main areas: (1) osmotic/pH regulation, (2) aerobic and hypoxic metabolism, (3) cell division and (4) protein regulation. In the absence of oxygen, energy production is converted to glycolytic fermentation, a process that produces excess H<sup>+</sup>, resulting in a decrease in pH upon emergence (Fan et al., 1991). While this seems consistent with the weight loss observation due to aerial exposure that accumulates H<sup>+</sup> ions, our gene expression data show that the SLA92 gene responsible for eliminating acids produced by active metabolism in pH regulation is most downregulated. This may be explained by the large reduction in metabolic rate and small change in weight loss, where metabolism is suppressed to cope with oxygen deprivation and lack of food availability.

Given such environmental constraints, various metabolic processes are up and downregulated. Specifically, macromolecule is upregulated in contrast to lipid, carbohydrate and cellular aldehyde. Unlike *Mytilus galloprovincialis* that mobilizes lipid as the principal source of energy to cope with a higher metabolic rate in air (Andrade et al., 2017), *M. virgatus* increases their protein and nucleic acids content possibly through producing antioxidant defense enzymes to combat oxidative damage while maintaining a lower metabolic rate. Histone acetylation is also downregulated to repress gene expression correspondingly. Consistent with Gracey et al.'s (2008) finding that the gene expression profiles of *Mytilus californianus* experiencing tidal changes reveal distinct physiological states that correspond to metabolism phase and cell-division phase, *M. virgatus* also display changes in cell division processes due to tidal

changes as evidenced by upregulation of nuclear genes at cell division sites and membrane regions.

However, while protein phosphorylation is upregulated to coordinate cell communication, signal transduction, cell apoptosis and other stress-related pathways, secondary protein processing, known as glycosylation, that modulates protein structure, function and stability and takes place in the endoplasmic reticulum is downregulated. Glycosylation is often coupled with the expression of heat shock proteins in molluscs facing different environmental stress, including changes in temperature, oxygen level, salinity and contaminant concentrations (Monari et al., 2011). Previous studies have documented the stimulation of heat shock response in aerial exposure without thermal stress, indicating that hypoxia by itself is sufficient to induce the expression of Hsp70 and Hsp90 in *M. galloprovincialis* (Anetis et al., 2019). However, unlike heated animals in the warming rate experiments, control mussels do not show changes in the expression of any heat shock proteins, indicating that other proteins are at play in regulating the physiological response to aerial exposure in *M. virgatus*.

## 4.2 Impact of Warming Rates

### 4.2.1 Rapid Stress Response

While the relationship between mollusc physiology and increasing temperatures is well documented, for example higher limpet heart rates (Marshall and McQuaid, 1992; Chelazzi and Williams, 1999) and increasing osmotic concentrations (Williams and Morritt, 1995; Williams et), the effect of warming rate up to a sublethal temperature has only been recently investigated. Moyen et al. (2019) examined two cardiac variables—the critical temperature at which heart rate drops rapidly ( $T_{crit}$ ) and flatline temperature at which heart rate drops to zero (FLT) at fast, moderate and slow rates. They concluded that only  $T_{crit}$  significantly increased with faster rates, but not FLT, inferring  $T_{crit}$  as a more physiologically plastic trait. Investigating the rapid stress response (T0-T1) and acclimation response (T1-T2), our study reveals that of the four physiological variables, only weight loss percentage and average thermal equilibrium vary significantly across heating rates. While weight loss percentage increases between fast and mid as well as fast and slow rates, average thermal equilibrium remains higher at slow rate compared to both fast and mid rates. Desiccation stress is positively correlated with both the degree and duration of heat exposure (Connell, 1961; Wolcott, 1973; Williams and Morritt, 1995). Since all rates expose mussels to the same maximal temperature, they differ in the duration of heat stress. With the fast rate reaching 40°C in a shorter period of time, it results in a smaller weight loss percentage. However, the shortened duration also implies that mussels are not as well acclimated to the high temperature as the slow rate. Therefore, their body temperatures dropped quickly in

comparison to mussels at the slow rate where they remained relatively close to 40°C even though thermographs were taken at room temperature.

Based on previous studies on thermal tolerance of terrestrial ectotherms, heating rates have varying effects on physiological indicators such as maximum critical temperature at which an organism starts losing locomotor abilities ( $CT_{max}$ ). Santos et al. (2012) and Casta et al. (2015) have found faster rates are correlated with higher  $CT_{max}$  while Chidawanyika et al. (2010) and Terblanche et al. (2011) concluded a negative relationship or no relationship at all respectively. A possible explanation is that the directionality of the relationship between heating rate and thermal tolerance is species and habitat dependent (Allen et al., 2012). Another explanation is that the relationship depends on which physiological markers are used to define thermal tolerance as different traits represent different resolutions of plasticity. For example, Moyen et al.'s (2019) findings that only  $T_{crit}$  but not FLT was different across heating rates reflect that  $T_{crit}$  is a more acutely plastic trait to be influenced by a transient abiotic factor such as heating rate. FLT, in contrast, would be more likely to be altered by chronic factors such as heat acclimatization. These suggest that heating rate is a more minute abiotic factor as compared to other variables such as absolute maximum temperature and that heart rate and osmolality may not have the same resolution to reflect the effect of heating rates even though they have been typical physiological indicators of thermal stress in many studies (Williams et al., 2011).

Given the lack of physiological significance across heating rates, molecular level analysis might better reflect the underlying effects of thermal stress. As temperature increases, there is considerable heat-induced damage to cells. Heat shock proteins (HSP) have been well known for its role to confer conformational stability to cellular proteins as chaperons to defend against anoxia and heat in many organisms including molluscs (Velazquez and Linquist, 1984; David et al., 2005; Gracey et al., 2008). The onset of HSP formation is evidence of the capacity of cells to control the amount of thermal damage by upregulating expression levels of HSP (Moyen et al., 2019). While HSP71 is expressed across all three warming rates, the mid rate has the highest average level of expression during the rapid stress response. This indicates that *M. virgatus* is most adapted to the mid rate of thermal change as it is the average ecological rate observed in the field (Williams et al., unpublished data).

Across all three rates, the fast rate has all the three upregulated genes related with protein folding function (BIP, DNJB1 and HSP71) to counter the rapid intense stress of heating whereas the mid (DNJB1 and HSP71) and slow rates only have two (DJNB and HSP71). Our results support Gracey et al.'s (2008) findings that the expression of protein-folding genes significantly correlates with proteotoxic stress from heating and serves as a primary protective function against heat stress. Faster rates are likely to induce more severe proteotoxic stress that leads to unfolding and dysfunctioning of essential proteins and upregulating protein chaperons helps

temporarily maintain protein integrity and function. In contrast, more pro-survival genes are exclusively upregulated at mid and slow rates, including transcriptional regulation (MS3L1), synaptic transmission to preserve postsynaptic signals and neural pathways (DLGP1) and cell adhesion for cell communication and maintenance of tissues (CO6A5). Moreover, only the fast rate increases the expression of C1QT3 that negatively regulates inflammatory response, suggesting that mussels are unable to mount repair mechanisms to slow down cellular damage under the short period of time.

In contrast to the common set of upregulated genes shared across rates, the variety of uniquely downregulated genes between all three rates suggests that they mobilize different molecular mechanisms at the expense to upregulate important processes, such as protein folding, in response to thermal stress. In particular, the fast rate has 4 downregulated genes related to immune response (CASP1, FIBA, IFIH1 and TLR6) while both the mid (JAK2) and slow rates (FIBA) only have one downregulated immune response gene. The downregulation of immune-related genes at the fast rate suggests a compromise of the organism's ability to counteract the non-lethal stress (Malagoli et al., 2007). In contrast, many of the top downregulated genes of mid and slow rates are distributed across different molecular functions, such as protein degradation, apoptosis inhibition, histone acetylation, cell division and embryonic patterning amongst others.

#### 4.2.2 Acclimation Response

While heating rate directly affects the rapid stress response, it is also a strong component of thermal acclimation response as the extent to which the mussels are capable of withstanding the sublethal temperature for a prolonged duration reflects how well they could cope with the specific heating rate. Increasing environmental temperatures have been correlated with elevated heart rates and increased metabolism to meet higher physiological needs and energy demands (Williams et al., 2005; Williams et al, 2011). During the acclimation phase, the mussels instead display a significantly reduced heart rate, indicating a sign of metabolic adjustment despite the high temperature. Weight loss percentage, on the other hand, increases over time as desiccation stress intensifies when mussels are continually being held at high heat for a prolonged duration. Moreover, average thermal equilibrium is also statistically higher during the acclimation response compared to the rapid stress response, indicating a sign of acclimation to the high temperature. However, osmolality does not have any statistically significant changes between the two timepoints. None of the four physiological variables show any significant relationship across heating rates during the acclimation phase, relating to the low resolution of such physiological indicators to reflect the effect of heating rate.

This sign of acclimation is also reflected in changes in gene expression between the two timepoints, with genes downregulated during the rapid stress response returning to higher expression levels. Three of these genes (IFIH1, JAK2 and GIMA4) fall under immune response and apoptosis inhibition that cover all three rates. The upregulation of immune-related genes and decline of apoptosis indicates an acclimation to the chronic heat stress by mounting pro-cell survival mechanisms (Kvitt et al., 2016) Moreover, in contrast to the rapid stress response where HSP71 is upregulated in most instances across rates, there are no further significant changes in its expression levels between both shore populations and across rates in the acclimation response. As HSP gene expression has been shown in other studies to represent non-specific response to stress (Li et al., 2008), the lack of any further upregulation of HSP genes reinforces an acclimation response to the prolonged heat stress. Since HSP71 is still continually expressed at similar levels and not down regulated, these mussels are not recovering from thermal stress, but have stabilized their molecular chaperons to maintain protein homeostasis. Unlike Podrabsky and Somero's (2004) findings that HSP transcripts in killifish were mildly induced during temperature cycling but strongly upregulated under chronic heat stress, our results indicates that rapid heating but not the duration of thermal stress is a precursor to the induction of HSP-related genes. Consistent with Li et al.'s (2010) finding that this chaperone gene is not triggered by any stress condition, HSP regulation thus provides a signature for the type of heat-induced stress—rapid heating or chronic elevated temperature stress (Place et al., 2008).

The effects of rates on the molecular responses to thermal stress can be observed during the acclimation response as there are gene expression patterns that change across rates. An interesting pathway that is differentially expressed across rates is apoptosis inhibition. Apoptosis is programmed cell death that removes damaged cells to maintain tissue homeostasis. Overexpression of apoptosis cell death will result in excess cell loss and functional impairment of tissue (Eefting et al., 2004). It could be activated by temperature-induced DNA damage (Richier et al., 2006) or accumulation of reactive oxygen species (ROS) production (Wu et al., 2018). GIMA4 is a GTPase immune-associated proteins family gene (GIMA4) that has important roles in supporting T-cell development, survival, homeostasis, autoimmunity and leukemogenesis, thereby playing a role in the regulation of apoptosis (Nitta and Takahama, 2007). Its upregulation at the slow rate inhibits apoptosis, suggesting less cellular damage and a potential recovery from the rapid heating during acclimation. This is consistent with the downregulation of XDH that is responsible for ROS generation. In contrast, the fast rate downregulates GIMA4 and upregulates GHITM that promotes mitochondrial apoptosis. The activation of apoptotic-related pathways indicates a trigger of apoptotic cell death, possibly related to the increased DNA damage from the upregulation of RS27A that activates the transcription factor NF-kappa-B. The inflammatory regulator NF-kappa-B has been shown to be tightly linked with the induction of apoptosis in other bivalve species, such as *Mytilus edulis* and *Crassostrea gigas* (Falfushynska et al., 2020). The opposite regulatory patterns of genes related

to cellular damage and apoptosis inhibition between rates suggests that the differential effects of rates on molecular responses to thermal stress persists through the acclimation phase. Specifically, the fast rate results in upregulation of genes related to thermal stress, such as protein folding and cellular injury, whereas the mid and slow rates result in upregulation of pro-survival pathways, such as immune response and apoptosis inhibition.

### 4.3 Adaptive Capability of Shore Populations

Vertical distribution has been found to vary in heat tolerance, with upper thermal limit increasing from lower to higher intertidal populations (Ngyuen et al., 2011). This is likely because high-shore mussels often experience faster heating rate and a greater range of body temperatures than low-shore mussels (Miller and Dowd, 2017). From an evolutionary perspective, it is advantageous for high-shore populations to improve their thermal tolerance at faster heating rates. As a result, the site-specific average daily heating rate determines the acclimation state and hence thermal tolerance of high and low shore mussels (Moyen et al., 2019). Studies such as Sorte et al. (2020) and Moyen et al. (2019) have found that higher shore populations have higher thermal or lethal tolerances. Moyen et al. (2019), in particular, concluded that high shore mussels have significantly higher  $T_{crit}$  than low-zone mussels across all warming rates, with the largest difference at the fast rate. In contrast, in our study, none of the four physiological variables investigated show any statistically significant differences between the two shore populations. This may be explained by the nature of these physiological indicators as being gross morphological characteristics. For example, Moyen et al. (2019) explained that the lack of difference in percentage water loss between the high and low zones during heating implied that the  $T_{crit}$  differences are likely not a result of osmotic stress, but molecular changes enabling improved cardiac thermal tolerance of high-shore mussels at faster heating rates.

Investigating the molecular mechanisms behind physiological performance may therefore reveal the subtle differences in thermal stress regulation between high and low shore populations. In particular, one of the most well-studied molecular markers of thermal stress, HSP70, has been found to be expressed at significantly higher levels in high-shore *M. californianus* compared to their low-shore conspecifics (Roberts et al., 1997; Gracey et al., 2008). Our results, however, show that this relationship of HSP71 differential expression between the shore populations, with higher expression in the high-shore population, is dependent on heating rate. High-shore mussels only show higher expression than low-shore mussels at fast and mid rates, but the comparison is reversed at the slow rate. As higher constitutive levels of HSP71 indicate a greater ability to ameliorate the heat-induced cellular damage, the similarly high HSP71 expression of high-shore mussels at both fast and mid rates suggests they are better coped than at the slow rate. On the contrary, the low-shore population does not significantly upregulate the HSP71 gene, but another similar protein-folding gene DNJB responsible for HSP40, at the fast rate and expresses slightly

lower levels of HSP71 at the mid rate. Instead, they have the highest HSP expression at the slow rate, illustrating an opposite trend compared to the high-shore population. HSP40 is a co-chaperon from the J-protein family that is required to initiate the ATPase activity of HSP70s (Kampinga and Craig, 2010). However, they alone only modestly stimulate HSP70 activity and other substrates are also required for synergistic binding to significantly upregulate HSP70 ATP hydrolysis rate (Kityk et al., 2018; Faust and Rosenzweig, 2020). The lack of upregulation of HSP70 and the upregulation of DNJB1 as a substitutive chaperon in the low-shore population may signal that they are unable to mount the main molecular chaperons in a short period of time and instead resort to a suboptimal substitute to maintain protein homeostasis. The difference in HSP expression pattern between the shore populations may be explained by their differential adaptive capability given their thermal acclimation history to different heating rates as a function of mussel shore height, supporting our hypothesis that high shore mussels tolerate faster heating rates better.

During rapid stress response, apart from HSP71, other genes are also uniquely and differentially regulated, suggesting that the high and low shore populations have different molecular mechanisms of thermoregulation in response to warming rates. Compared to the high-shore population, the low-shore mussels significantly downregulate immune-related genes (e.g. CASP, FIBA and TLR6) at the fast rate, suggesting that the rapid heating negatively impacts their immune function to thermal stress. This immunosuppression can lend mussels more susceptible to increased levels of bacterial infection, reducing their fitness for survival (Lacoste et al., 2001; Bussell et al., 2008). In contrast, the high-shore population tends to upregulate genes for histone acetylation (e.g. CO6A5, MS3L1) at mid and slow rates whereas the low-shore population upregulates genes pertaining to protein folding and apoptosis inhibition, which are upregulated by high-shore population at the fast rate. This temporal lag of upregulating protein folding and anti-apoptosis genes between the two shore populations at different rates suggests that there is a common sequence of expression profiles following initial heat shock, depending on the thermal acclimation state of the mussels to the experimental warming rate. The upregulation of histone acetylation genes may confer the high-shore population enhanced stress resistance and hence long-term selective survival advantage as Zhou et al. (2019) have shown that histone acetylation elevated by heat exposure results in the long-lasting expression of defense response genes.

This differential gene expression pattern of different molecular functional pathways between the two shore populations persists through the acclimation phase. The high-shore population upregulates genes related to cell cycle and proliferation (e.g. CALM and UBC9) at mid and slow rates whereas the low-shore population downregulates such genes (e.g. SAM9L, LAP2 and RAE1L). Place et al. (2008) showed that in contrast to the positive correlation between sea surface temperature and mussel growth established in previous studies, aerial body temperature can negatively affect growth in *M. californianus*'s population. Our results further suggest that

warming rate affects organismal growth differentially in different shore populations, with greater negative impact on lower shore population. This can be seen in the delay and arrest of cellular growth and proliferation of the low-shore population to cope with the higher energetic costs induced by thermal stress (Place et al., 2008). Furthermore, the upregulation of DUT for nucleotide metabolism and the downregulation of ODO2 for carbohydrate metabolism by the low-shore population at the fast rate indicates a further switch from aerobic to anaerobic metabolism as the extended period of stress incurs additional metabolic costs. While oxygen deficiency causes aerobic metabolism to cease and switch to anaerobic metabolism, prolonged thermal and desiccation stress further drives the imbalance between energy production and energy utilization (Jennings and Steenbergen, 1985). Given that anaerobic glycolysis produces less than 10% of oxidative phosphorylation, the upregulation of anaerobic metabolism suggests that the low-shore population has not fully coped with the ATP consumption required to withstand the rapid heating induced by the fast rate. As such, our results show that while the two shore populations do not display significantly different physiological responses, the high-shore population may have a higher thermal tolerance due to higher protein folding gene expression, faster signaling activation and transduction as well as stronger repair and immune ability against heat stress.

#### 4.4 Coupling of Physiological and Genetic Mechanisms

The non-statistical significance of heart rate and osmolality across rates and between shore populations suggests that inter-individual variation is greater than treatment differences. As reported by Moyen et al. (2019), both high and low-shore mussels experience a similar large range of  $T_{crit}$  of 7.2 and 6.7°C. This large interindividual variability in physiological responses may be explained by the large range of heating rates experienced within both high and low shore mussel beds, which range up to 14.7 and 10.8°C h<sup>-1</sup> respectively as reported by Miller and Dowd (2017). Further work by Miller and Dowd (2019) found that the temperature extremes were similar at both tidal heights and that individuals within the same mussel bed can vary drastically in physiological status and past history from its nearby neighbours, differing by as much as 14°C of body temperature at low tide among mussels separated by centimeters. The huge inter-individual variation in heart rates and other physiological traits within the same shore population may therefore be a result of a huge variability in thermal acclimation to warming rates within the same mussel bed.

However, our genetic analysis has identified genes that may denote the effects of rates and shore populations on thermal performance based on differential expression profiles of various important functional pathways. These mainly fall under protein folding, cell cycle regulation, metabolism, apoptosis inhibition and immune response. While we surveyed overall transcriptional profile changes, potential links between these molecular functional pathways

could be established with physiological responses. For example, minute differences in organismal physiology are reflected in the metabolic adjustment at the molecular level, such as the increase in heart rate of low-shore population between the rapid stress and acclimation responses at the fast rate may correlate with the upregulation of anaerobic metabolic gene, denoting a higher energetic cost. Similarly, the lack of up or downregulation of any osmoregulatory gene provides support for the insignificant differences in osmolality across rates and between tidal shores. This is consistent with Falfushynska et al.'s (2020) conclusion that the lack of correlation between tissue oxidative injury and activation of apoptotic pathways during hypoxia shows that oxidative stress is not the major mechanism for inducing cellular stress response. As such, the overall transcriptional profile differences not only serve to explain the physiological trends, but also seem to provide a higher resolution to elucidate the differences in regulatory mechanisms governing the effects of rates on thermal stress response between shore populations.

Finally, it should be noted that the inter-individual variation observed in physiological traits of thermal tolerance may also be a result of genetic polymorphism rather than simply a result of a mosaic of environmental conditions. Han (2020) found that inter-individual variations in heat tolerance correlate significantly with variations in specific genetic loci, with heterozygotes exhibiting higher tolerance than homozygotes. Under balancing selection, thermally resistant *M. virgatus* heterozygotes survive to balance the loss of homozygotes during mass mortalities in summer, resulting in seasonal changes in genotype frequency. Microhabitat heterogeneity in temperature and genetic variations thus act in concert to maintain genetic polymorphism for the resistance to thermal stress. Consequently, correlation between physiological and genetic traits should be established with consideration of both differences in genetic composition of shore populations and environmental variation along the intertidal rocky shore.

## 5. CONCLUSIONS

Our study provides the first description to link physiological and molecular level responses of tropical intertidal organisms to a specific abiotic factor of thermal stress—the effect of warming rate. Overall, the interactive effects of being emersed and the rate of warming have shown that mussels respond differently at the molecular and physiological levels to these scenarios. While heart rate and osmolality amongst the physiological responses do not appear to vary significantly across warming rates, weight loss percentage and average thermal equilibrium as well as gene expression profiles display different patterns that largely support the hypothesis of this study. Faster rates induce intense stress over a shortened period of time, resulting in smaller weight loss and lower acclimation to high temperature. To cope with the higher energetic costs, stress-related pathways, such as protein folding, are upregulated at the expense of pro-survival pathways such as cell cycle regulation. On the contrary, slow rates extend the stress over a longer duration, resulting in greater weight loss but higher acclimation to thermal equilibrium, allowing mussels to upregulate pro-survival pathways such as apoptosis inhibition and immune response in a more controlled manner.

Moreover, we have investigated whether this thermoregulation differs between shore populations. High-shore population with greater plasticity to a larger range of warming rates displays greater upregulation of heat shock proteins at the fast rate and activates immune response and cell cycle regulation at mid and slow rates. Low-shore population, in contrast, upregulates heat shock proteins at mid and slow rates but downregulates immune response at the fast rate. The thermal performance and survival of intertidal marine organisms may, therefore, be dependent on both the warming rates and thermal acclimatization state based on tidal height. As high-shore populations live close to their upper thermal tolerance limits (Somero, 2010), our study has illustrated that warming rate is one such physiological system that affects populations' acclimatization capacities for adjusting their thermal tolerances and may explain why mass mortalities often occur at the upper boundary of mussel beds during hot summers. Molecular approaches can contribute to physiological studies by providing insights into how protein-coding genes and gene regulatory mechanisms influence organismal capacities to respond to acute and long-term temperature rises at different warming rates. Using a combination of molecular and physiological approaches will elucidate the strategies intertidal organisms employ to survive in the physically challenging environment of tropical rocky shores.

## 6. RECOMMENDATIONS

As noted by Moyen et al. (2019), the relationship between warming rate and thermal tolerance of mussels depends on their acclimatization states that are determined by both mean daily warming rates in the site and absolute maximum temperatures reached during emersion. These thermal variables are likely to differ between shore populations. As such, experimental warming rates in the laboratory should be selected based on the mean daily warming rate within each tidal height instead of testing across the same absolute range to allow for ecologically relevant conclusions. Unfortunately, we were unable to obtain temporal profiles of warming rates in the site between shore populations before commencement of the experiments in summer. However, we selected the absolute warming rates based on the mean heating rate across the mussel bed from unpublished data and other studies on warming rates for marine ectotherms. Additionally, we employed 3 temperature loggers per tidal height to record the temperature and warming rate variations within the mussel bed for further analysis. We would expect that our results yield ecologically relevant insights on the relationship between warming rates and thermal tolerance.

As discussed previously, the large inter-individual variation observed in physiological traits, such as heart rate, may be a result of their low resolution to reflect the effect of a transient abiotic factor—warming rate on thermal tolerance. Future work should therefore focus on other proxies of metabolic rates, such as oxygen consumption, carbon dioxide production or ATP turnover rate. Biochemical assays and protein mass spectroscopy profiling can also offer detailed insights into the activity of biological molecules relating to specific physiological components. Apart from the resolution of the physiological traits, the large variation may be attributed to a small sample size. For example, heart rate measurements for some replicates have to be discarded since there are no regular heartbeats detected (Figure S3). Moreover, due to financial constraints, only 3 samples per treatment were sent for RNA sequencing. The low number of replicates may have amplified the inter-individual variation and result in lower resolution. Finally, due to time and computing resource constraints, we were only able to do a preliminary *de novo* gene assembly by pooling from 5 samples, possibly affecting the quality of the consensus genome constructed since not all transcripts expressed in all samples are covered. The lack of a genome reference additionally made functional annotation more challenging. Further genetic analysis will be conducted to elucidate various aspects of differential gene expression across rates and between tidal heights, such as functional pathways, alternative splicing, gene isoforms and multifunctional genes.

Despite such limitations, our work still lends important insights into the functional and molecular mechanisms of thermal stress regulation of intertidal marine organisms at different warming rates. As the first study that attempts to reveal the fine-scale biogeographic variation in thermoregulation and acclimation to heating rates, our results will serve to inform how physiological and cellular mechanisms are co-regulated by the rate of temperature change. Our

work attempts to elucidate how environmental signals such as air temperatures may be translated into signals at the cellular scale of the organism to yield important insights into the interaction of the functional and molecular regulation of thermal response in intertidal ectotherms when exposed to air. As such, our results may explain biological phenomena related to thermal tolerance, for example *Mytilus edulis*' summer mass mortality under recurrent heat stress (Sueront et al., 2019). Given the threat of climate change and vulnerability of tropical marine ectotherms to temperature rise, understanding the molecular and physiological responses of intertidal mussels such as ecosystem engineer *M. virgatus*, becomes increasingly important to predict the possible impacts of global warming on marine ectotherms (Somero, 2005; Helmuth et al., 2006; Hofmann and Todgham, 2010).

Future directions for research in this area may include conducting intra-individual comparison by tracking changes in physiological and molecular responses within the same individual. As the larger inter-individual variation in physiological performance may be a result of environmental mosaic within the rocky shore habitat, performing intra-individual analysis can characterize an individual's thermal background and respective conditions within the habitat. This may provide important insights on whether the impacts of future climate change may be highly specific to individuals based on their relative microhabitat within the mosaic (Miller and Dowd 2019). Correlation between genotypic and physiological traits that determine the individual's unique thermal history and performance in their disparate micro-environments can also be established by investigating specific thermoregulatory genes using quantitative techniques such as qPCR. However, challenges remain with genotyping thermal stress response profiles within the same individual since animals need to be killed for tissue extraction. Furthermore, as *M. virgatus* seems to cope well with 40°C of body temperature in the short term, another possible future direction is to further stress the animals to a higher maximum temperature extreme since higher temperatures may reflect better regulation of stress. Finally, spatial comparison of thermoregulation can be done by sampling different populations to examine whether the responses are generalised for the species across latitudinal gradients or influenced by local conditions.

## ACKNOWLEDGEMENTS

I would like to extend my sincerest gratitude to my research mentors, Juan Diego Gaitán-Espitia and Gray A. Williams, for giving me the opportunity to work on this project and their unwavering support throughout the research process from ideation to experimentation to data analysis. I would also like to thank Martin Cheng for providing his tremendous help in designing and setting up the tanks, collecting mussels from Shek O, Hong Kong and conducting the heat ramping experiments. I am also grateful for members in both the Integrative Biology & Evolutionary Ecology Research Group (iBEER) and the Tropical Intertidal Ecology Group (TIDE), including but not limited to Bovern Suchart Arromrak, Tommy Hui, Adrian Wong and Cecily Leung, for lending laboratory equipment and assisting me in navigating through laboratory administration at HKU. Additionally, I would like to thank my project advisor, Hugh Ducklow, for his guidance and constructive feedback throughout the writing process with my thesis, presentation and poster. Finally, I would like to thank Women Divers' Hall of Fame's Marine Conservation Scholarship, Columbia's Ecology, Evolution and Environmental Biology Departmental Funding and Columbia College Senior Thesis Funding for financially supporting this research.

## SUPPLEMENTARY FIGURES



Figure S1. Acclimation tank setup in wet laboratory



Figure S2. Warming water baths for the heating experiments

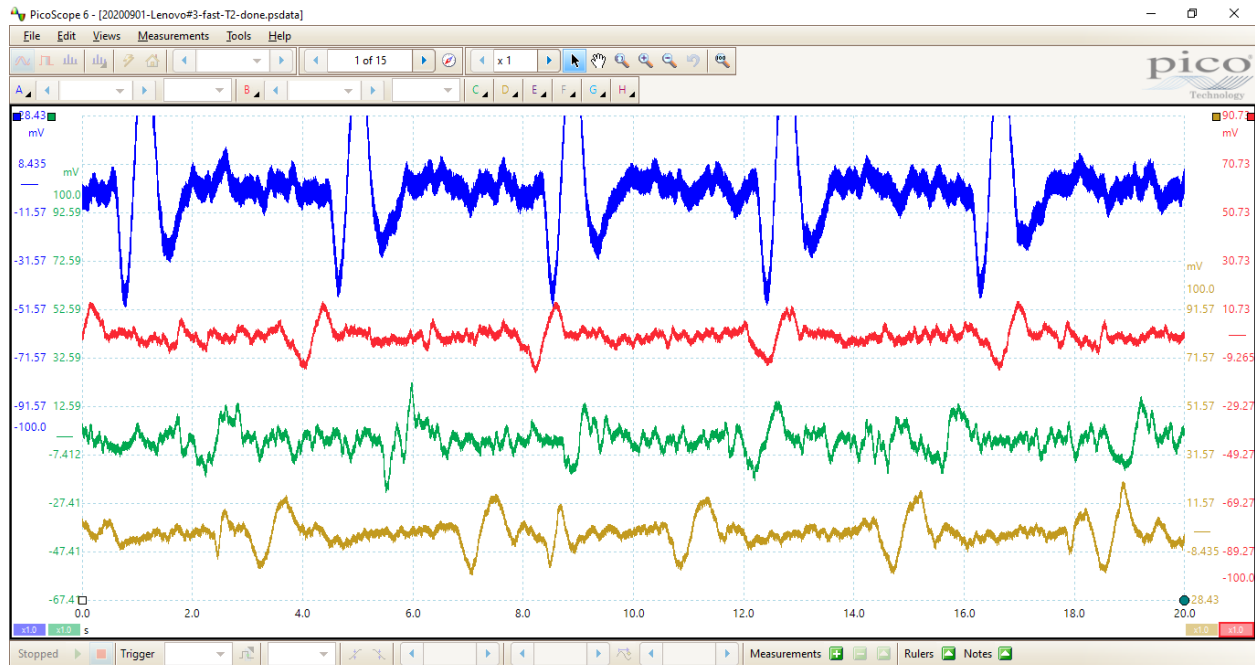


Figure S3. Sample heart rate pattern for analysis using Picoscope software

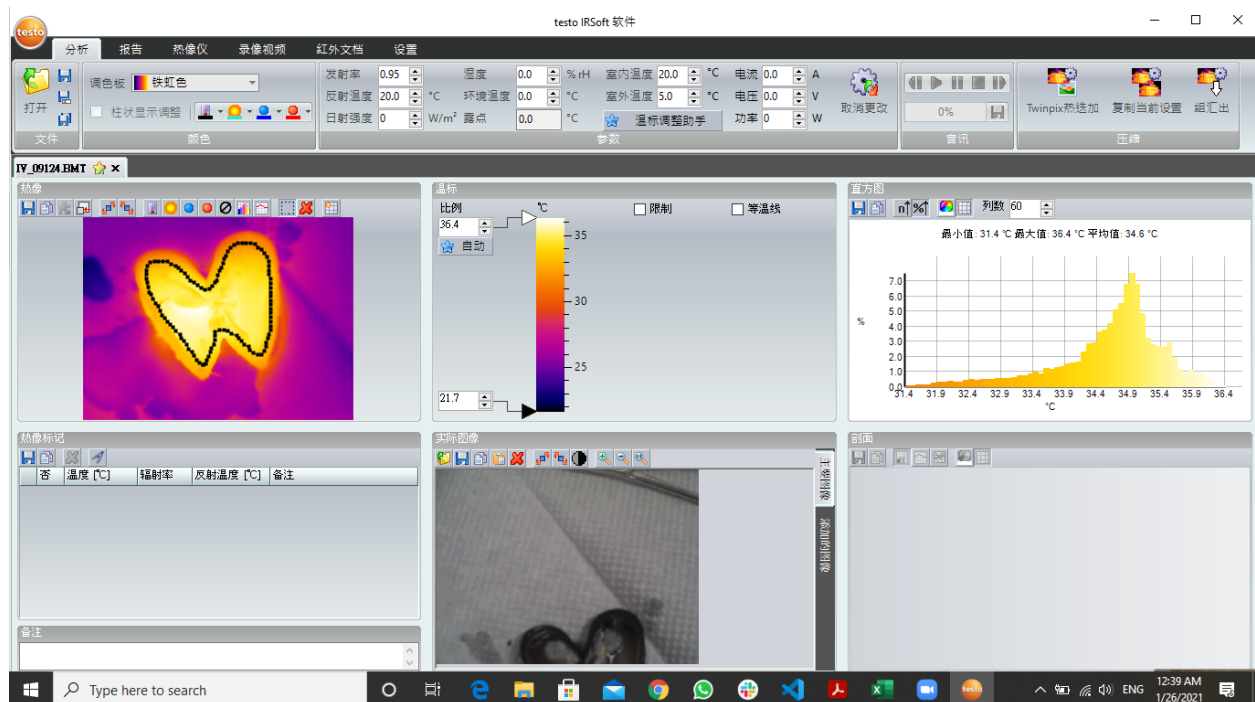


Figure S4. Sample thermal camera picture for analysis using Testo Software

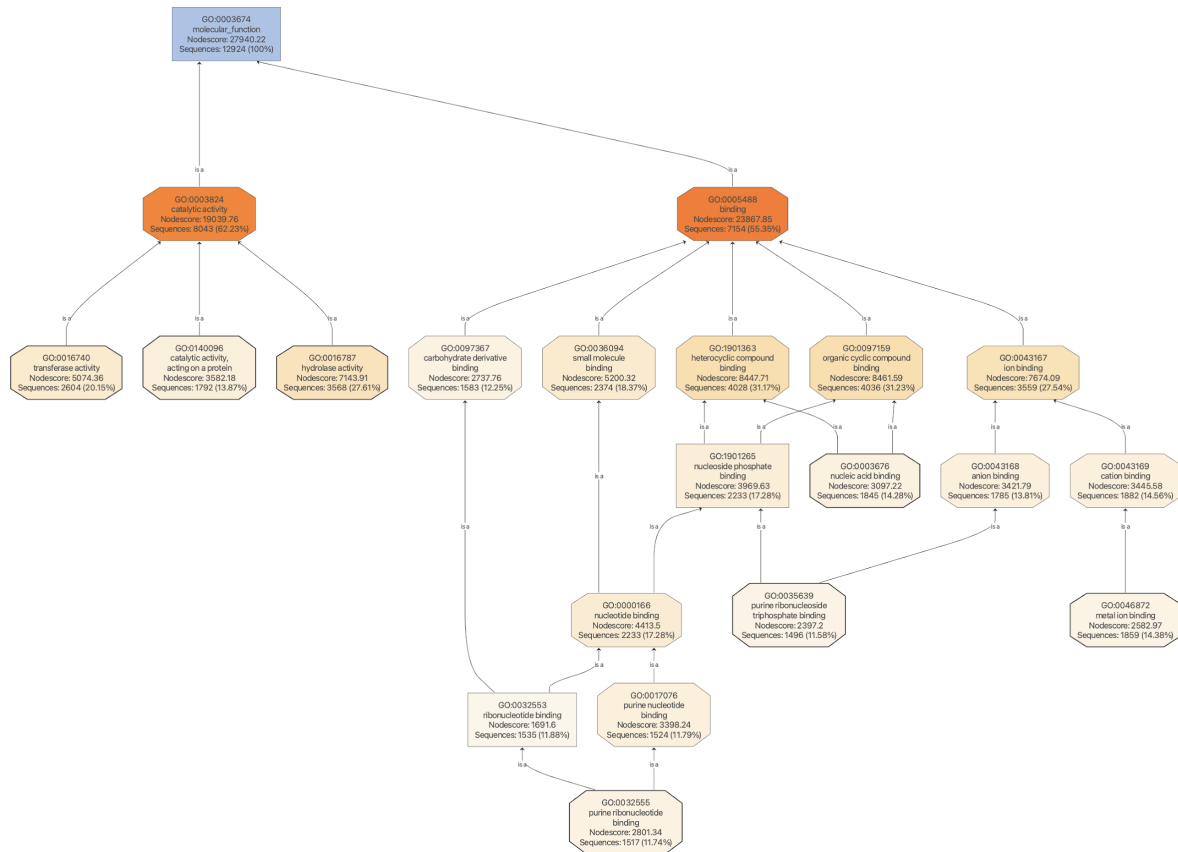


Figure S5. Distribution of transcripts relating to molecular function using GO annotation

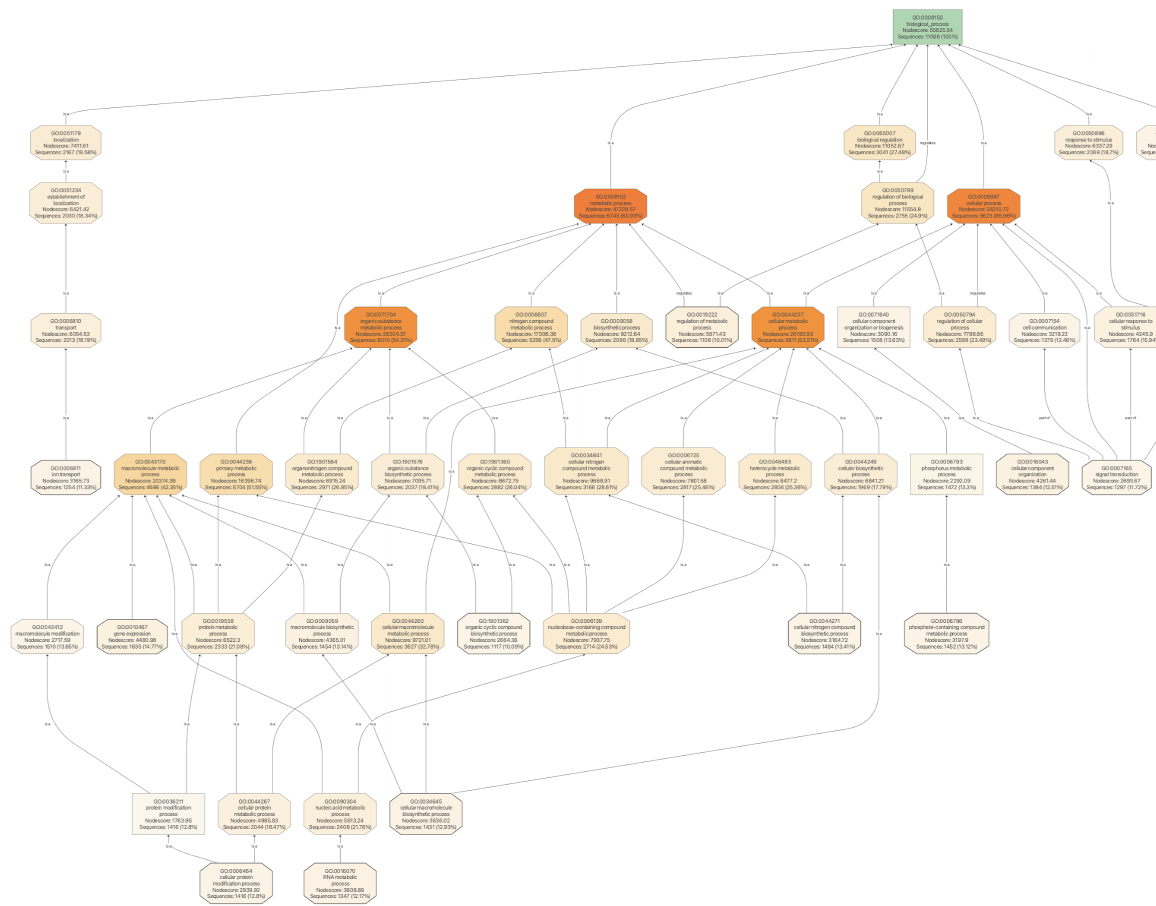


Figure S6. Distribution of transcripts relating to biological processes using GO annotation

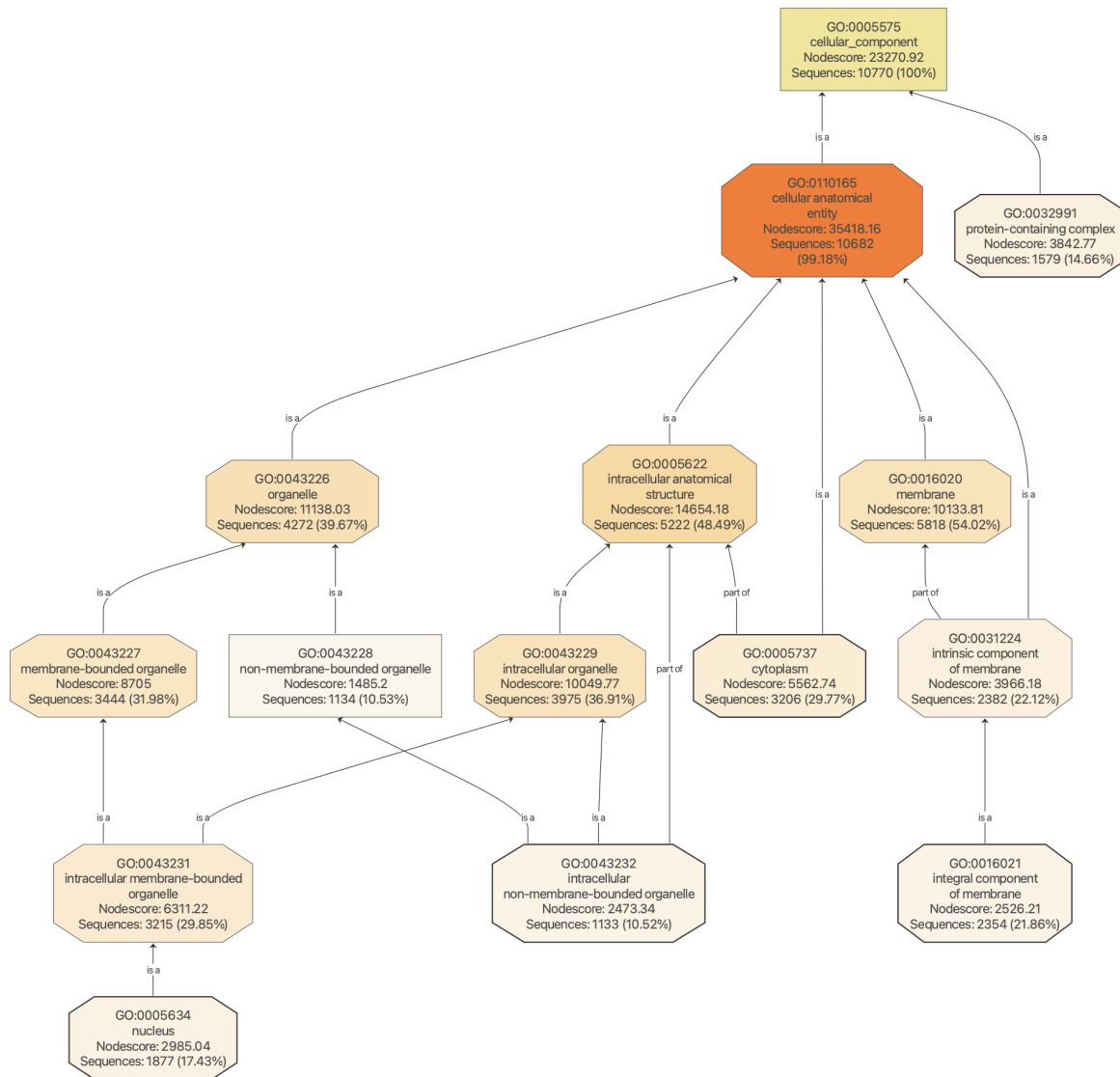


Figure S7. Distribution of transcripts relating to cellular components using GO annotation

**SUPPLEMENTARY TABLES**

Table S1. Pivot table showing the number of replicates for each physiological variable

<i>heating_rate</i>	<i>time_point</i>	<i>tidal_height</i>	COUNT of heart_rate	COUNT of osmolality	COUNT of weight_loss_percent	COUNT of average_temp
+ Total			0	0	0	0
- C_air	- T0	H	2	4	4	3
		L	4	4	3	3
	T0 Total		6	8	7	6
C_air Total			6	8	7	6
- C_water	- T0	H	2	3	3	3
		L	2	3	3	3
	T0 Total		4	6	6	6
C_water Total			4	6	6	6
- F	- T1	H	5	6	6	4
		L	6	6	6	4
	T1 Total		11	12	12	8
	- T2	H	6	5	6	4
		L	6	6	6	4
	T2 Total		12	11	12	8
F Total			23	23	24	16
- M	- T1	H	6	6	6	4
		L	4	6	6	4
	T1 Total		10	12	12	8
	- T2	H	6	6	6	4
		L	6	6	6	4
	T2 Total		12	12	12	8
M Total			22	24	24	16
- S	- T1	H	3	4	4	4
		L	4	4	4	4
	T1 Total		7	8	8	8
	- T2	H	3	4	4	4
		L	4	4	4	4
	T2 Total		7	8	8	8
S Total			14	16	16	16
<b>Grand Total</b>			<b>69</b>	<b>77</b>	<b>77</b>	<b>60</b>

Table S2. Data quality summary of 24 *M. vigatus* samples sequenced

Sample	Raw reads	Raw data	Effective(%)	Error(%)	Q20(%)	Q30(%)	GC(%)
C11L	51224496	7.7	96.73	0.03	97.92	93.55	35.33
C2H	44232260	6.6	96.98	0.03	97.64	93.20	34.17
C7H	43731400	6.6	96.31	0.03	97.90	93.45	34.10
C4H	44891460	6.7	96.91	0.03	97.69	93.02	34.51
C14L	50831792	7.6	97.28	0.03	97.76	93.11	34.51
C19L	45159130	6.8	96.27	0.03	97.80	93.33	34.58
C5H	48056852	7.2	97.00	0.03	97.82	93.26	35.19
F36L	51582170	7.7	97.19	0.03	97.78	93.19	35.30
S59H	55520550	8.3	95.94	0.03	97.58	93.35	35.73

F35L	51820954	7.8	97.41	0.03	97.47	92.54	35.25
S69L	43339438	6.5	97.34	0.03	97.60	92.96	35.22
M55L	40448632	6.1	96.86	0.03	97.68	92.98	35.57
S65H	43795704	6.6	97.11	0.03	97.53	93.07	35.78
M53L	47448480	7.1	97.54	0.03	97.64	92.89	35.08
S63H	44579206	6.7	96.66	0.03	97.72	93.12	35.46
F29H	50890236	7.6	96.72	0.03	97.56	92.70	35.12
F27H	45174918	6.8	97.45	0.03	97.75	93.12	35.14
F34L	41541168	6.2	98.08	0.02	98.15	94.17	35.41
M42H	48415520	7.3	97.60	0.03	97.77	93.14	34.52
M46H	46262660	6.9	96.83	0.03	97.72	93.09	35.68
M51L	44035732	6.6	97.56	0.03	97.62	92.75	34.99
S67L	48028692	7.2	96.82	0.03	97.52	93.07	35.20
F37L	43330644	6.5	96.18	0.03	97.55	92.63	35.53
M44H	48869042	7.3	97.31	0.03	97.95	93.57	35.44
F26H	42390272	6.4	96.53	0.03	97.59	92.77	35.64
F28H	42654562	6.4	97.75	0.03	97.63	92.85	35.23
M54L	45992060	6.9	96.93	0.03	97.82	93.31	35.10
C18L	48132970	7.2	96.80	0.03	97.09	91.52	34.20
F24H	48235468	7.2	97.53	0.03	97.68	92.98	34.97
S71L	41420556	6.2	97.72	0.03	97.61	92.78	35.26
S66H	45380256	6.8	97.60	0.03	97.73	93.05	34.65
F33L	47507440	7.1	96.56	0.03	97.59	93.14	35.49
M47H	45137582	6.8	97.92	0.03	97.62	92.84	35.33
F30H	54122278	8.1	96.67	0.03	97.46	92.52	35.29
S74L	47299894	7.1	96.50	0.03	97.71	93.40	35.40
M56L	46049920	6.9	97.42	0.03	97.65	92.93	35.41
S64H	45460918	6.8	97.33	0.03	97.65	92.95	35.75
S62H	44278194	6.6	97.68	0.03	97.68	92.92	35.44
S73L	43343080	6.5	96.45	0.03	97.75	93.49	36.12
F31L	47487204	7.1	97.19	0.03	97.75	93.10	34.69
M45H	49126602	7.4	96.72	0.03	97.64	92.84	35.74
S70L	44913756	6.7	97.44	0.03	97.62	92.83	34.96

M50L	47168236	7.1	97.41	0.03	97.32	92.20	34.83
M48H	46971282	7.0	97.86	0.03	97.80	93.19	34.94

Table S3. Top 5 upregulated and downregulated genes of each shore population across all rates with absolute log fold change > 1.5 and p-value < 0.01

Rate	Shore	Time	Regulation	Genes	logFC	logCPM	F	PValue	
High	T0 vs T1		Up	SSH2.1	12.30	6.83	8.35	0.0065	
				HSP71.3	11.92	6.41	8.85	0.0062	
				CO6A5.4	10.14	4.12	15.49	0.0004	
				BIP.7	9.94	3.81	9.09	0.0050	
			Down	MS3L1.1	9.87	4.40	13.86	0.0007	
				ITPR1.3	-11.01	4.73	7.79	0.0083	
	T1 vs T2		Down	RENT1.1	-10.93	4.74	8.16	0.0072	
				XIAP.22	-10.75	6.38	7.92	0.0078	
				BP10.4	-10.41	4.69	9.11	0.0046	
				PREP.2	-9.81	4.42	10.02	0.0033	
			Up	XIAP.22	11.37	6.38	9.11	0.0046	
Slow	T1 vs T2			BP10.4	10.25	4.69	9.19	0.0045	
				FCN2.2	9.95	3.49	8.14	0.0071	
				CALM.30	9.68	3.85	7.56	0.0096	
				PREP.2	9.10	4.42	9.07	0.0049	
		Down	BRPF1.5	-10.67	4.87	8.94	0.0054		
	T0 vs T1				HOOK3.2	-9.76	4.22	7.79	0.0083
					C1D.1	-9.50	4.14	8.04	0.0074
					NAS39.3	-9.43	1.90	8.44	0.0089
					HS12A.3	-9.38	2.81	9.10	0.0046
Low	T0 vs T1		Up	HSP71.3	12.80	6.41	10.22	0.0036	
				DLGP1.1	12.14	5.95	7.89	0.0080	
				PTC1.2	11.45	4.81	17.01	0.0002	
				RADI.1	11.14	5.40	9.07	0.0048	
			Down	PIAP.5	10.41	5.98	8.37	0.0065	
	T1 vs T2			DCMC.1	-12.04	4.48	7.75	0.0085	
		Down	FIBA.8	-11.15	4.63	7.73	0.0091		
			FICD.2	-10.98	4.42	9.01	0.0048		
			RAE1L.3	-10.63	3.65	10.28	0.0031		
		Up	PANG1.2	-10.33	3.80	8.60	0.0058		
	T1 vs T2				RSSA.1	13.35	7.46	8.96	0.0049
					ACTP1.6	10.84	3.48	10.49	0.0027
					FICD.2	10.15	4.42	8.10	0.0072
					GIMA4.7	9.64	3.76	9.60	0.0037
					GIMA4.6	9.57	5.76	7.44	0.0098
			Up	PIAP.4	-11.51	5.18	7.88	0.0080	
				SAM9L.4	-10.91	6.04	8.03	0.0075	
				LAP2.1	-10.10	4.50	9.09	0.0047	
			Down	BTBD2.2	-9.75	3.33	12.23	0.0013	
				XDH.1	-9.59	0.81	8.52	0.0076	

Rate	Shore	Time	Regulation	Genes	logFC	logCPM	F	PValue
High	T0 vs T1	Up	HSP71.3	13.19	6.41	10.52	0.0032	
			SSH2.1	12.13	6.83	8.14	0.0072	
			MS3L1.1	10.56	4.40	15.59	0.0004	
			TIF1A.3	10.56	4.24	11.71	0.0017	
		Down	CO6A5.4	10.52	4.12	16.50	0.0003	
	T1 vs T2		MS3L1.2	-10.59	4.03	11.32	0.0020	
			JAK2.1	-10.53	4.66	9.60	0.0037	
			LZTR1.2	-10.20	3.65	8.45	0.0071	
			LEO1.3	-9.78	4.63	8.75	0.0054	
			POL5.32	-9.57	2.12	8.40	0.0065	
Mid	T0 vs T1	Up	UBC9.1	10.04	4.80	8.23	0.0071	
			MS3L1.2	9.80	4.03	10.24	0.0031	
			CHRD1.2	9.46	3.15	12.65	0.0011	
			LEO1.3	9.39	4.63	8.42	0.0063	
		Down	JAK2.1	9.04	4.66	7.50	0.0095	
	T1 vs T2		TITIN.13	-11.18	2.94	11.41	0.0021	
			MTSS1.3	-11.16	5.70	7.56	0.0098	
			RTXE.14	-9.40	3.11	12.58	0.0011	
			POL3.85	-8.96	2.99	8.86	0.0053	
			CO8A1.1	-8.76	2.21	10.57	0.0028	
Low	T0 vs T1	Up	HSP71.3	12.06	6.41	9.25	0.0052	
			DLGP1.1	11.82	5.95	7.54	0.0094	
			DNJB1.3	11.39	4.52	13.72	0.0007	
			PIAP.5	10.85	5.98	9.03	0.0048	
		Down	PTC1.2	10.82	4.81	15.49	0.0004	
	T1 vs T2		LZTR1.2	-10.09	3.65	8.18	0.0080	
			SL9A2.2	-9.77	5.59	9.32	0.0043	
			PLMN.30	-9.64	1.32	10.44	0.0034	
			IP6K3.1	-8.74	1.06	7.86	0.0084	
			POL5.23	-8.13	2.51	11.03	0.0020	
High	T0 vs T1	Up	HS12A.75	11.92	6.06	9.07	0.0049	
			ATLA1	11.35	4.61	8.42	0.0064	
			C1QL3.3	10.90	4.60	10.30	0.0028	
			SL9A2.2	10.61	5.59	11.39	0.0018	
		Down	LPH.11	10.52	1.66	12.90	0.0010	
	T1 vs T2		BRPF1.5	-10.80	4.87	9.11	0.0050	
			PDLI5.2	-10.57	5.00	7.92	0.0085	
			MUT7.2	-10.30	4.66	12.86	0.0010	
			RBM4B.3	-10.03	4.82	12.13	0.0014	
			RAE1L.3	-9.84	3.65	9.52	0.0043	

Rate	Shore	Time	Regulation	Genes	logFC	logCPM	F	PValue
High	T0 vs T1	Up	HSP71.3	13.07	6.41	10.36	0.0034	
			SSH2.1	11.81	6.83	7.77	0.0085	
			C1QT3.4	10.35	5.76	9.97	0.0031	
			BIP.7	10.28	3.81	9.62	0.0040	
			TIF1A.3	10.09	4.24	10.84	0.0024	
	T1 vs T2	Down	VWDE.16	-12.58	7.38	10.14	0.0030	
			DYHG.1	-10.33	5.46	8.37	0.0064	
			G2E3.7	-10.02	2.77	7.59	0.0096	
			IFIH1.6	-9.96	4.41	14.04	0.0007	
			NID2.5	-9.01	6.82	8.19	0.0068	
Fast	T0 vs T1	Up	VWDE.16	13.33	7.38	11.52	0.0017	
			GHITM.1	11.06	4.57	8.03	0.0076	
			DYHG.1	10.04	5.46	8.23	0.0068	
			IFIH1.6	9.94	4.41	14.51	0.0006	
			WGE.1	9.46	3.64	7.74	0.0085	
	T1 vs T2	Down	DLGP1.2	-11.86	6.50	7.72	0.0086	
			TADBP.1	-10.16	4.30	21.69	0.0000	
			GIMA4.7	-9.50	3.76	7.85	0.0081	
			RBM4B.3	-9.48	4.82	10.91	0.0022	
			RETR3.1	-9.47	3.73	7.81	0.0085	
Low	T0 vs T1	Up	EFCB6.4	11.62	5.32	28.17	0.0000	
			RADI.1	11.56	5.40	9.65	0.0037	
			PIAP.5	11.37	5.98	9.80	0.0035	
			DNJB1.3	10.09	4.52	11.23	0.0019	
			PTC1.2	9.93	4.81	13.37	0.0008	
	T1 vs T2	Down	FIBA.8	-11.15	4.63	8.01	0.0080	
			TTC37.1	-10.02	4.29	8.13	0.0071	
			CASP1.1	-9.55	2.74	7.57	0.0095	
			FIBA.7	-9.45	2.91	7.96	0.0082	
			TLR6.2	-9.12	1.49	7.65	0.0091	
High	T0 vs T1	Up	TANC2.2	10.86	2.19	14.02	0.0021	
			ATLA1	10.68	4.61	7.76	0.0086	
			SHANK.2	10.43	4.13	8.90	0.0053	
			DUT.2	8.32	2.35	9.63	0.0037	
			RS27A.1	8.25	2.46	11.08	0.0019	
	T1 vs T2	Down	MTSS1.3	-12.07	5.70	8.45	0.0066	
			PTPRT.18	-11.66	5.76	7.81	0.0082	
			SAHH2.1	-10.28	4.24	8.24	0.0076	
			ODO2.2	-9.96	4.69	10.57	0.0025	
			PININ.2	-9.66	3.87	8.68	0.0056	

## REFERENCES

- Alcántara, A. R., M-J. Hernaiz, and J-V. Sinisterra. "Biocatalyzed production of fine chemicals." (2011): 309-331.
- Allen, J. L., Chown, S. L., Janion-Scheepers, C., & Clusella-Trullas, S. (2016). Interactions between rates of temperature change and acclimation affect latitudinal patterns of warming tolerance. *Conservation Physiology*, 4(1), 1–14. <https://doi.org/10.1093/conphys/cow053>
- Angilletta, M. J., Cooper, B. S., Schuler, M. S., & Boyles, J. G. (2010). The evolution of thermal physiology in ectotherms. *Frontiers in Bioscience - Elite*, 2 E(3), 861–881. <https://doi.org/10.2741/e148>
- Biggar, K. K., and K. B. Storey. (2015). Insight into post-transcriptional gene regulation: stress-responsive microRNAs and their role in the environmental stress survival of tolerant animals. *The Journal of Experimental Biology* 218:1281–1289.
- Biggar, K. K., and K. B. Storey. (2018). Functional impact of microRNA regulation in models of extreme stress adaptation. *Journal of Molecular Cell Biology* 10:93–101.
- Clark, M. S., Sommer, U., Sihra, J. K., Thorne, M. A. S., Morley, S. A., King, M., ... Peck, L. S. (2017). Biodiversity in marine invertebrate responses to acute warming revealed by a comparative multi-omics approach. *Global Change Biology*, 23(1), 318–330. <https://doi.org/10.1111/gcb.13357>
- Denny, M. W., Miller, L. P., & Harley, C. D. G. (2006). Thermal stress on intertidal limpets: Long-term hindcasts and lethal limits. *Journal of Experimental Biology*, 209(13), 2420–2431. <https://doi.org/10.1242/jeb.02258>
- Denny, M. W., Dowd, W. W., Bilir, L., & Mach, K. J. (2011). Spreading the risk: small-scale body temperature variation among intertidal organisms and its implications for species persistence. *Journal of Experimental Marine Biology and Ecology*, 400(1-2), 175-190.
- Falfushynska, H., Piontkivska, H., & Sokolova, I. M. (2020). Effects of intermittent hypoxia on cell survival and inflammatory responses in the intertidal marine bivalves *Mytilus edulis* and *Crassostrea gigas*. *Journal of Experimental Biology*, 223(4). <https://doi.org/10.1242/jeb.217026>
- Freire, C. A., A. F. Welker, J. M. Storey, K. B. Storey, and M. Hermes-Lima. (2011). Oxidative stress in estuarine and intertidal environments (temperate and tropical). Pages 41–57 *Oxidative stress in aquatic ecosystems*.

Gleason, Lani U., et al. "Plasticity of thermal tolerance and its relationship with growth rate in juvenile mussels (*Mytilus californianus*)."*Proceedings of the Royal Society B: Biological Sciences* 285.1877 (2018): 20172617.

González, K., Gaitán-Espitia, J., Font, A., Cárdenas, C. A., & González-Aravena, M. (2016). Expression pattern of heat shock proteins during acute thermal stress in the Antarctic sea urchin, *Sterechinus neumayeri*. *Revista Chilena de Historia Natural*, 89, 1–9.  
<https://doi.org/10.1186/s40693-016-0052-z>

Gracey, A. Y., Chaney, M. L., Boomhower, J. P., Tyburczy, W. R., Connor, K., & Somero, G. N. (2008). Rhythms of gene expression in a fluctuating intertidal environment. *Current Biology*, 18(19), 1501-1507.

Guppy, M., & Withers, P. (1999). Metabolic depression in animals: physiological perspectives and biochemical generalizations. *Biological Reviews*, 74(1), 1-40.

Hadj-Moussa, H., J. A. Moggridge, B. E. Luu, J. F. Quintero-Galvis, J. D. Gaitán-Espitia, R. F. Nespolo, and K. B. Storey. (2016). The hibernating South American marsupial, *Dromiciops gliroides*, displays torpor-sensitive microRNA expression patterns. *Scientific Reports* 6.

Haider, F., Falfushynska, H. I., Timm, S., & Sokolova, I. M. (2020). Effects of hypoxia and reoxygenation on intermediary metabolite homeostasis of marine bivalves *Mytilus edulis* and *Crassostrea gigas*. *Comparative Biochemistry and Physiology -Part A : Molecular and Integrative Physiology*, 242(January), 110657. <https://doi.org/10.1016/j.cbpa.2020.110657>

HAN, G., WANG, W., & DONG, Y. (2020). Effects of balancing selection and microhabitat temperature variations on heat tolerance of the intertidal black mussel *Septifer virgatus*. *Integrative Zoology*, 1–12. <https://doi.org/10.1111/1749-4877.12439>

Helmuth, B. S. T., & Hofmann, G. E. (2001). Microhabitats, thermal heterogeneity, and patterns of physiological stress in the rocky intertidal zone. *Biological Bulletin*, 201(3), 374–384.  
<https://doi.org/10.2307/1543615>

Helmuth, B., Broitman, B. R., Blanchette, C. A., Gilman, S., Halpin, P., Harley, C. D. G., ... Strickland, D. (2006). Mosaic patterns of thermal stress in the rocky intertidal zone: Implications for climate change. *Ecological Monographs*, 76(4), 461–479.  
[https://doi.org/10.1890/0012-9615\(2006\)076\[0461:MPOTSI\]2.0.CO;2](https://doi.org/10.1890/0012-9615(2006)076[0461:MPOTSI]2.0.CO;2)

Helmuth, B., Russell, B. D., Connell, S. D., Dong, Y., Harley, C. D., Lima, F. P., ... Mieszkowska, N. (2014). Beyond long-term averages: making biological sense of a rapidly

- changing world. *Climate Change Responses*, 1(1).  
<https://doi.org/10.1186/s40665-014-0006-0>
- Koch, L. (2017). A thermometer controlling gene expression. *Nature Reviews Genetics* 18:515.
- Liu and Morton. (n.d.). The temperature tolerances of *Tetraclita squamosa* and *Septifer virgatus* on a sub-tropical rocky shore in Hong Kong.
- Lockwood, B. L., Sanders, J. G., & Somero, G. N. (2010). Transcriptomic responses to heat stress in invasive and native blue mussels (genus *Mytilus*): Molecular correlates of invasive success. *Journal of Experimental Biology*, 213(20), 3548–3558.  
<https://doi.org/10.1242/jeb.046094>
- Logan, C. A., Kost, L. E., & Somero, G. N. (2012). Latitudinal differences in *Mytilus californianus* thermal physiology. *Marine Ecology Progress Series*, 450, 93-105.
- Marshall, D. J., & McQuaid, C. D. (1993). Differential physiological and behavioural responses of the intertidal mussels, *Choromytilus meridionalis* (Kr.) and *Perna perna* L., to exposure to hypoxia and air: a basis for spatial separation. *Journal of Experimental Marine Biology and Ecology*, 171(2), 225–237. [https://doi.org/10.1016/0022-0981\(93\)90005-9](https://doi.org/10.1016/0022-0981(93)90005-9)
- McAfee, D., Bishop, M. J., Yu, T. N., & Williams, G. A. (2018). Structural traits dictate abiotic stress amelioration by intertidal oysters. *Functional Ecology*, 32(12), 2666–2677.  
<https://doi.org/10.1111/1365-2435.13210>
- Miller, L. P., & Dowd, W. W. (2017). Multimodal in situ datalogging quantifies inter-individual variation in thermal experience and persistent origin effects on gaping behavior among intertidal mussels (*Mytilus californianus*). *Journal of Experimental Biology*, 220(22), 4305-4319.
- Miller, L. P., & Dowd, W. W. (2019). Repeatable patterns of small-scale spatial variation in intertidal mussel beds and their implications for responses to climate change. *Comparative Biochemistry and Physiology Part A: Molecular & Integrative Physiology*, 236, 110516.
- Millhouse, S., & Manley, J. L. (2005). The C-terminal domain of RNA polymerase II functions as a phosphorylation-dependent splicing activator in a heterologous protein. *Molecular and cellular biology*, 25(2), 533–544. <https://doi.org/10.1128/MCB.25.2.533-544.2005>
- Morritt, D., Leung, K. M. Y., Pirro, M. De, Yau, C., Wai, T. C., & Williams, G. A. (2007). Responses of the limpet, *Cellana grata* (Gould 1859), to hypo-osmotic stress during

- simulated tropical, monsoon rains. *Journal of Experimental Marine Biology and Ecology*, 352(1), 78–88. <https://doi.org/10.1016/j.jembe.2007.07.002>
- Morton, B. (n.d.). The population dynamics and reproductive cycle of *Septifer virgatus* on an exposed rocky shore in Hong Kong.
- Nguyen, K. D. T., Morley, S. A., Lai, C. H., Clark, M. S., Tan, K. S., Bates, A. E., & Peck, L. S. (2011). Upper temperature limits of tropical marine ectotherms: Global warming implications. *PLoS ONE*, 6(12), 6–13. <https://doi.org/10.1371/journal.pone.0029340>
- Niehaus, A. C., Angilletta, M. J., Sears, M. W., Franklin, C. E., & Wilson, R. S. (2012). Predicting the physiological performance of ectotherms in fluctuating thermal environments. *Journal of Experimental Biology*, 215(4), 694–701. <https://doi.org/10.1242/jeb.058032>
- Pinsky, M. L., Eikeset, A. M., McCauley, D. J., Payne, J. L., & Sunday, J. M. (2019). Greater vulnerability to warming of marine versus terrestrial ectotherms. *Nature*, 569(7754), 108–111. <https://doi.org/10.1038/s41586-019-1132-4>
- Rolán-Alvarez, E., C. J. Austin, and E. G. Boulding. (2015). The contribution of the genus littorina to the field of evolutionary ecology. *Oceanography and Marine Biology: An Annual Review* 53:157–214.
- Rossi, F., Palombella, S., Pirrone, C., Mancini, G., Bernardini, G., & Gornati, R. (2016). Evaluation of tissue morphology and gene expression as biomarkers of pollution in mussel *Mytilus galloprovincialis* caging experiment. *Aquatic Toxicology*, 181(2016), 57–66. <https://doi.org/10.1016/j.aquatox.2016.10.018>
- Rozen-Rechels, D., Dupoué, A., Lourdais, O., Chamaillé-Jammes, S., Meylan, S., Clobert, J., & Le Galliard, J. F. (2019). When water interacts with temperature: Ecological and evolutionary implications of thermo-hydroregulation in terrestrial ectotherms. *Ecology and Evolution*, 9(17), 10029–10043. <https://doi.org/10.1002/ece3.5440>
- Shick, J. M., De Zwaan, A., & De Bont, A. T. (1983). Anoxic metabolic rate in the mussel *Mytilus edulis* L. estimated by simultaneous direct calorimetry and biochemical analysis. *Physiological Zoology*, 56(1), 56–63.
- Shumway, S. E., & Freeman, R. F. H. (1984). Osmotic balance in a marine pulmonate, *Amphibola crenata*. *Marine & Freshwater Behaviour & Phy*, 11(2), 157–183.

- Sokolova, I. M., Bock, C., & Pörtner, H. O. (2000). Resistance to freshwater exposure in White Sea *Littorina* spp. I: Anaerobic metabolism and energetics. *Journal of Comparative Physiology B*, 170(2), 91-103.
- Sorte, C. J., Bernatchez, G., Mislan, K. A. S., Pandori, L. L., Silbiger, N. J., & Wallingford, P. D. (2019). Thermal tolerance limits as indicators of current and future intertidal zonation patterns in a diverse mussel guild. *Marine Biology*, 166(1), 1-13.
- Storey, K. B. (2015). Regulation of hypometabolism: insights into epigenetic controls. *Journal of Experimental Biology* 218:150–159.
- Storey, K. B., and J. M. Storey. (2004). Metabolic rate depression in animals: transcriptional and translational controls. *Biological Reviews* 79:207–33.
- Storey, K. B., and J. M. Storey. (2005). Oxygen Limitation and Metabolic Rate Depression. Pages 415–442 *Functional Metabolism*.
- Storey, K. B., and J. M. Storey. (2010). Aestivation. Pages 25–45 *Aestivation: Molecular and Physiological Aspects*, *Progress in Molecular and Subcellular Biology*.
- Tagliarolo, M., & McQuaid, C. D. (2015). Sub-lethal and sub-specific temperature effects are better predictors of mussel distribution than thermal tolerance. *Marine Ecology Progress Series*, 535(September 2015), 145–159. <https://doi.org/10.3354/meps11434>
- Tagliarolo, M., & McQuaid, C. D. (2016). Field measurements indicate unexpected, serious underestimation of mussel heart rates and thermal tolerance by laboratory studies. *PLoS ONE*, 11(2). <https://doi.org/10.1371/journal.pone.0146341>
- Tomanek, L., & Zuzow, M. J. (2010). The proteomic response of the mussel congeners *Mytilus galloprovincialis* and *M. trossulus* to acute heat stress: Implications for thermal tolerance limits and metabolic costs of thermal stress. *Journal of Experimental Biology*, 213(20), 3559–3574. <https://doi.org/10.1242/jeb.041228>
- Vinagre, C., Leal, I., Mendonça, V., & Flores, A. A. V. (2015). Effect of warming rate on the critical thermal maxima of crabs, shrimp and fish. *Journal of Thermal Biology*, 47, 19–25. <https://doi.org/10.1016/j.jtherbio.2014.10.012>
- WetHEY, D. S., Woodin, S. A., Hilbish, T. J., Jones, S. J., Lima, F. P., & Brannock, P. M. (2011). Response of intertidal populations to climate: Effects of extreme events versus long term change. *Journal of Experimental Marine Biology and Ecology*, 400(1–2), 132–144. <https://doi.org/10.1016/j.jembe.2011.02.008>

Williams, G. A., & Morritt, D. (1994). Habitat partitioning and thermal tolerance in a tropical limpet, *Cellana grata*. *Marine Ecology Progress Series*, 124, 89–103.

Williams, G. A., De Pirro, M., Cartwright, S., Khangura, K., Ng, W. C., Leung, P. T. Y., & Morritt, D. (2011). Come rain or shine: The combined effects of physical stresses on physiological and protein-level responses of an intertidal limpet in the monsoonal tropics. *Functional Ecology*, 25(1), 101–110. <https://doi.org/10.1111/j.1365-2435.2010.01760.x>

Wijenayake, S., B. E. Luu, J. Zhang, S. N. Tessier, J. F. Quintero-Galvis, J. Gaitán-Espitia, R. F. Nespolo, and K. B. Storey. (2018). Strategies of biochemical adaptation for hibernation in a South American marsupial *Dromiciops gliroides*: 1. Mitogen-activated protein kinases and the cell stress response. *Comparative Biochemistry and Physiology Part - B: Biochemistry and Molecular Biology*.